

Conditions on holographic entangling surfaces in higher curvature gravity

Johanna Erdmenger, Mario Flory and Charlotte Sleight

*Max-Planck-Institut für Physik (Werner-Heisenberg-Institut),
Föhringer Ring 6, D-80805, Munich, Germany*

E-mail: jke@mpp.mpg.de, mflory@mpp.mpg.de, csleight@mpp.mpg.de

ABSTRACT: We study the extremal surfaces of functionals recently proposed for the holographic calculation of entanglement entropy in general higher curvature theories, using New Massive gravity and Gauss-Bonnet gravity as concrete examples. We show that the entropy functionals admit closed extremal surfaces, which for black hole backgrounds can encircle the event horizon of the black hole. In the examples considered, such closed surfaces correspond to a lower value of the entropy functional than expected from CFT calculations, implying a seeming mismatch between the bulk and boundary calculations. For Lorentzian settings we show that this problem can be resolved by imposing a causality constraint on the extremal surfaces. The possibility of deriving conditions from an alternative conical boundary condition method as proposed by Lewkowycz and Maldacena is explored.

Contents

1	Introduction	1
2	Functional prescriptions of holographic entanglement entropy	4
3	Significance of closed extremal surfaces	6
4	Extremal curves in New Massive gravity	8
4.1	NMG and proposed entropy functional	8
4.2	Equations of motion of NMG entropy functional	9
4.3	Curves anchored at the boundary	10
4.4	Closed extremal curves in NMG	11
5	Closed extremal surfaces in Gauss-Bonnet gravity	14
6	Closed bulk extremal surfaces and the causal influence argument	16
7	Conical boundary condition method in Gauss-Bonnet gravity	21
8	Discussion	25
8.1	Summary	25
8.2	Outlook	27
9	Acknowledgements	29
A	Notation	29
B	Explicit equations of motion for the entropy functional in NMG	30
C	Closed extremal curves of other black hole solutions in NMG	31

1 Introduction

The concept of entanglement entropy has proven to be of great interest to the physics community in recent years. The search of a better understanding of quantum systems, in particular at criticality, has lead to the establishment of general analytic results for entanglement entropy in two-dimensional CFTs (see e.g. [1]), while in higher dimensions the study of entanglement entropy is less simple. Entanglement entropy also appears to be instrumental for a deeper understanding of holography [2, 3].

The development of an understanding of entanglement entropy in the framework of the AdS/CFT correspondence [4–6] is therefore of utmost interest. A simple example of the

AdS/CFT correspondence at play in this context is given by the Bekenstein-Hawking entropy [7, 8]

$$S_{BH} = \frac{\text{Area of Horizon}}{4G_N}, \quad (1.1)$$

which for BPS black holes has a microscopic derivation in string theory [9], implying a relation between gravitational entropy and the degeneracy of quantum field theory as its microscopic description. Important progress was made by Ryu and Takayanagi (RT) [10, 11], who generalised the Bekenstein-Hawking formula above to the holographic calculation of entanglement entropy in CFTs with Einstein-Hilbert gravity duals. Here, the entanglement entropy is given by the area of a minimal surface which is anchored to the given spatial region in the CFT. This prescription for entanglement entropy was recently proven by Lewkowycz and Maldacena in [12] by translating the replica trick to the classical gravity action in the bulk, and showing that the resultant prescription for holographic entanglement entropy is equivalent to that of RT. However to date there is no proof of its covariant generalisation by Hubeny, Rangamani and Takayanagi (HRT) [13].

More recently, generalisations of the RT and HRT formulae to general higher derivative theories of gravity have been proposed [14–17]. In black hole backgrounds, for consistency a correct prescription should reduce to Wald’s entropy functional [18–20]

$$S_{\text{Wald}} = -2\pi \int_{\mathcal{B}} d^{d-1}y \sqrt{\gamma} \frac{\partial L}{\partial R_{\mu\rho\nu\sigma}} \varepsilon_{\mu\rho} \varepsilon_{\nu\sigma}, \quad (1.2)$$

when evaluated on the black hole bifurcation surface \mathcal{B} (see appendix A for notation). Despite parallels to the Einstein-Hilbert case, Wald’s functional does not provide a prescription for the calculation of entanglement entropy in field theory duals to higher curvature gravity [21], and the current proposals take into account the extrinsic curvature of the surfaces upon which they are evaluated.

When using functionals to calculate entanglement entropy, they must be evaluated on a particular surface in the bulk anchored to the region of interest in the boundary CFT. One way to locate these surfaces could be to directly extremise the functionals, which has already been proposed in [16]. In this paper we investigate this method for static and partially static backgrounds (i.e. AdS and black hole backgrounds) in New Massive Gravity (NMG) and Gauss-Bonnet gravity, with a particular focus on the nature of the closed extremal surfaces of the corresponding functionals. In black hole backgrounds, a particularly important closed extremal surface is the black hole bifurcation surface. When evaluated on the black hole bifurcation surface, the entanglement entropy functional yields Wald’s formula (1.2) for black hole entropy. This coincides with the dual CFT entropy by standard AdS/CFT lore [22].

We find there exists an extra closed extremal surface for certain parameter ranges in NMG and Gauss-Bonnet gravity. Such surfaces can give a lower value for the entropy than that expected from CFT calculations. A prescription for calculating entanglement entropy based on only extremising the functionals would hence lead us to incorrectly equate the dual CFT entropy with that given by the additional closed extremal surface. Our findings lead us to conclude that, for consistency and physical values for entanglement entropy,

additional constraints on the extremal surfaces need to be imposed. In section 6 we show that in a covariant setting such constraints can be motivated by causality. For Euclidean settings, since causality cannot be used to derive constraints on the surfaces, in section 7 we investigate whether constraints can be derived by solving the equations of motion with conical boundary conditions.

Summary of results

The main findings of our paper can be summarised as follows: The functionals proposed for the calculation of holographic entanglement entropy in higher curvature gravities allow for extremal surfaces in addition to those that correspond to the correct physical value of entanglement entropy. We find that existing prescriptions for the holographic calculation of entanglement entropy are not sufficient, as in some cases they would lead one to incorrectly pick an unphysical additional surface as the one that is supposed to yield the CFT result. We examine examples of such additional surfaces in NMG and Gauss-Bonnet gravity. For Lorentzian settings we present an argument based on causality that can be employed to consistently eliminate the additional surfaces found. For Euclidean settings, we investigate the possibility of deriving conditions that entangling surfaces must satisfy by considering the extension of the replica trick into the bulk. The arguments we present for both Lorentzian and Euclidean settings can in principle be applied to any gravitational theory that admits asymptotically AdS solutions.

This paper is organised as follows: In section 2 we introduce static and covariant prescriptions for calculating entanglement entropy in both the Einstein-Hilbert and higher curvature gravity theories. For higher curvature gravity theories, we define these as the RT-like and HRT-like prescriptions, respectively. In section 3 we explain the significance of the closed extremal surfaces of holographic entanglement entropy functionals, in particular the role played by the homology constraint in the interpretation of such surfaces. In sections 4 and 5 we study the nature of the extremal surfaces of the entropy functionals in NMG and Gauss-Bonnet gravity, paying particular attention to their closed extremal surfaces in the bulk. We explain that in using the functionals to calculate entanglement entropy, constraints on the extremal surfaces additional to the homology constraint need to be imposed. In section 6, we introduce causality arguments which provide constraints in the covariant HRT-like prescription. In search of constraints for the static RT-like prescription, in section 7 we turn to an alternative method of locating extremal surfaces for entanglement entropy in static scenarios, first proposed by Lewkowycz and Maldacena [12]. In section 8 we summarise our results, and discuss their implications for functional prescriptions of entanglement entropy. Several lengthy details are relegated to the appendices: In appendix A we explain the notation used throughout the paper, and in appendix B the full form of the equation of motion studied in section 4 is given. In appendix C we briefly discuss extremal surfaces for the rotating BTZ and Lifshitz black holes of NMG.

While in the final stages of this project, we learned of a similar study [23] where it is investigated under which conditions there might be a clash between holographic prescriptions for computing relative entropy and the manifest positivity of this quantity in field theory terms.

2 Functional prescriptions of holographic entanglement entropy

Let us introduce the covariant and static functional prescriptions for the holographic calculation of entanglement entropy in Einstein-Hilbert gravity and general higher curvature theories. We utilise functional prescriptions for entanglement entropy throughout this paper, and only in section 7 is an alternative prescription discussed, which is based on extending the replica trick into the bulk. We refer to this alternative method as the *conical boundary condition method*.

For Einstein-Hilbert gravity, the Ryu-Takayanagi (RT) prescription provides a means of holographically calculating entanglement entropy in the static case: When the bulk spacetime \mathcal{M} with asymptotic boundary $\partial\mathcal{M}$ is static, there exists a timelike Killing vector field that induces a foliation of both \mathcal{M} and $\partial\mathcal{M}$ into spacelike surfaces. For a CFT region A on such a spacelike slice of the boundary $\partial\mathcal{M}$, the entanglement entropy \mathcal{S}_A associated with A is given by the area of the bulk minimal-area surface \mathcal{E}_A located on the same spacelike slice in the bulk via

$$\mathcal{S}_A = \frac{\text{Area}(\mathcal{E}_A)}{4G_N}, \quad (2.1)$$

where G_N is the gravitational constant. In this formula, \mathcal{E}_A is anchored to $\partial\mathcal{M}$, such that the intersection of \mathcal{E}_A with the boundary $\partial\mathcal{M}$ equals the boundary ∂A of the CFT-region A (figure 1). The bulk minimal surface is also required to satisfy the *homology condition*: there must exist a hypersurface \mathcal{F} in \mathcal{M} such that the boundary of \mathcal{F} is the union of \mathcal{E}_A and A [24]. \mathcal{E}_A is then said to be homologous to A ,¹ and we will refer to such surfaces as (*holographic*) *entangling surfaces*.

The Hubeny-Rangamani-Takayanagi (HRT) prescription extends RT to arbitrary time-dependent states, thus providing a covariant prescription for holographic entanglement entropy. More concretely, for a given spacelike CFT region A on the boundary $\partial\mathcal{M}$ of the asymptotically AdS spacetime, one searches for bulk surfaces \mathcal{E}_A anchored to $\partial\mathcal{M}$ which *extremise* the area functional, picking the surface that gives the smallest entropy:

$$\mathcal{S}_A = \min_X \frac{\text{Area}(\mathcal{E}_A)}{4G_N} \quad X = \{\mathcal{E}_A : \partial\mathcal{E}_A \equiv \mathcal{E}_A \cap \partial\mathcal{M} = \partial A\}. \quad (2.2)$$

It was recently noted in [25] that in order to obtain consistent results in certain bulk spacetimes, for example those with multiple bifurcation surfaces like the Reissner-Nordström black hole, the homology condition has to be either refined or appended with an additional causality condition. The authors of [25] imposed the additional constraint that the hypersurface \mathcal{F} is spacelike, as was already done by Wall in [26]. This seems to follow naturally from the RT approach, where \mathcal{F} is spacelike by construction.

Headrick, Hubeny, Lawrence and Rangamani in contrast obtain a causality constraint on the HRT prescription in [27, 28]. Primarily, this causality constraint demands that there

¹Note that in the static RT prescription \mathcal{F} is by construction located in the constant-time slice of \mathcal{M} .

should be no causal contact possible between \mathcal{E}_A and A .² This argument will be explained in more detail in section 6, and plays an instrumental role in the findings of this paper as it enables us to consistently rule out the unphysical additional surfaces in a Lorentzian setting. The fact that we can use this argument to exclude these surfaces is one of the main results of this work.

We will henceforth adopt the convention that the HRT prescription is based on the variation of the area functional using a general homology condition, as originally proposed in [13]. Whenever we make use of a refined homology condition or additional causality conditions, such as in section 6, we will explicitly mention this.

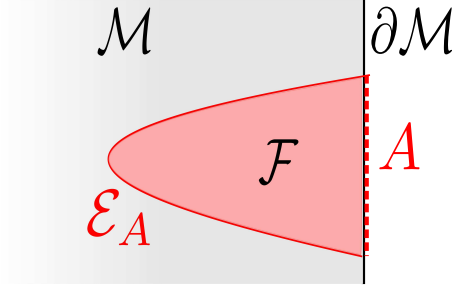


Figure 1. Setup for the calculation of the holographic entanglement entropy corresponding to the boundary region A . The time direction of \mathcal{M} (and $\partial\mathcal{M}$) is suppressed in this picture.

As mentioned in the introduction, for the holographic calculation of entanglement entropy in CFTs dual to higher curvature gravity theories, modified functionals have been proposed in [14–17]. In particular, for a general four-derivative theory of gravity with (Lorentzian) Lagrangian

$$S = \frac{1}{16\pi G_N} \int d^{d+1}x \sqrt{-g} \left[R + 2\Lambda + aR^2 + bR_{\mu\nu}R^{\mu\nu} + cR_{\mu\nu\alpha\beta}R^{\mu\nu\alpha\beta} \right], \quad (2.3)$$

the following functional was first derived in [14]:

$$\mathcal{S}_{EE} = \frac{1}{4G_N} \int_{\Sigma} d^{d-1}y \sqrt{\gamma} \left[1 + 2aR + b \left(R_{\parallel} - \frac{1}{2}k^2 \right) + 2c \left(R_{\parallel\parallel} - \text{Tr}(k)^2 \right) \right], \quad (2.4)$$

where Σ is a spacelike co-dimension two hypersurface, with induced metric γ_{ij} and extrinsic curvature terms k and $\text{Tr}(k)^2$. Further explanation for the notation used in this formula can be found in appendix A.

In using the entropy functionals (2.4) to calculate entanglement entropy of a given CFT region A holographically, a crucial step is to locate the particular co-dimension two surface anchored to ∂A in the bulk upon which the functional should be evaluated. Since for any

²It would be an interesting question to investigate when the causality constraint and the spacelike constraint on \mathcal{F} are equivalent. For example, it is conceivable that in a spacetime where closed timelike curves are created by identifying two spacelike slices it is impossible to satisfy the causality condition, while the demand that \mathcal{F} should be spacelike could still be easily met. The relation between these two possible conditions will be investigated in [28]. However we are not going to deal with causally pathological examples in this work, and we assume in the discussion of section 6 that both conditions could be used equivalently.

given A there is an infinite number of possible surfaces obeying the homology condition, a priori it is not clear which of these should be chosen. In principle it should be possible to determine the surface by solving all the equations of motion of the higher curvature theory with conical boundary conditions [12, 16], and this is demonstrated for Gauss-Bonnet gravity in section 7. However for a general higher curvature theory, in practice this calculation is very involved. As noted in [16], it would be advantageous to instead be able to determine the surface by directly extremising the functional. This was argued to be true for theories of the form (2.3) by comparing the equations of motion derived from extremising the functional with certain equations derived from the conical boundary condition method in [16]. In this paper we find that this method of locating the correct co-dimension two surfaces of the functional (2.4), for consistency and physicality, needs to be supplemented by constraints additional to the homology constraint on the extremal surfaces. Our conclusions are drawn by studying the nature of the extremal surfaces of the entropy functional (2.4) for (partially) static backgrounds in New Massive gravity [29, 30] and Gauss-Bonnet gravity [31, 32].

Let us introduce some definitions employed throughout this paper, which translate the RT and HRT prescriptions of Einstein-Hilbert gravity to general higher curvature theories. When extremising the entropy functional (2.4) on an equal time slice of a (partially) static spacetime, we refer to this as the *RT-like prescription*. In the *HRT-like prescription*, we need not restrict extremising the functional to equal time slices of the spacetime, as they may not be uniquely defined at all (e.g. when the extremal curves lie inside a black hole horizon as in section 4.4). Whenever using causality arguments that intrinsically depend on a covariant setting this will be referred to as an *HRT-like prescription amended with additional conditions*.

In Einstein-Hilbert gravity, for a (partially) static setting the RT prescription and the HRT prescription with additional conditions are believed to be equivalent. However in the higher curvature case, our findings show that when taking causality conditions into account, the RT- and HRT-like prescriptions do not agree at least in NMG and Gauss-Bonnet gravity and it is the HRT-like prescription amended with a causality constraint that gives the physically expected result, see section 6. We find these inconsistencies by investigating closed extremal surfaces of the entropy functionals in black hole and AdS backgrounds, whose significance we explain in the next section.

3 Significance of closed extremal surfaces

When calculating the entanglement entropy of a (small) subsystem of the whole boundary using the RT and HRT prescriptions, one needs to search for surfaces extremising the entropy functional that are anchored at the asymptotic boundary. But there may also exist extremal surfaces which are not anchored to the boundary, and instead form closed surfaces in the bulk. This is illustrated for the example of a black hole background in 2.

In [25, 34], for stationary black hole backgrounds in Einstein-Hilbert gravity it was shown that these closed extremal surfaces are very important: They are homologous to the full

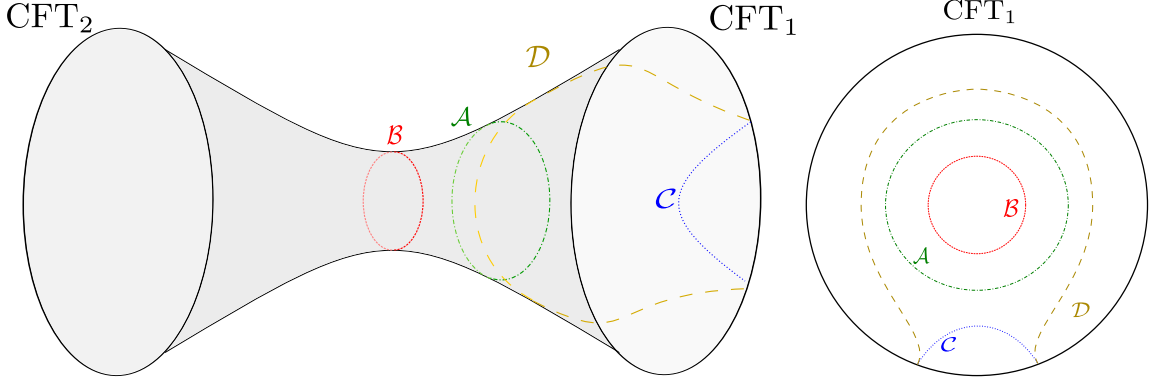


Figure 2. On the left side, we sketch a spacelike slice of a black hole spacetime with $t = \text{const.}$, also known as an Einstein-Rosen bridge. In a conformal diagram such as figure 3, this corresponds to a straight line through the center connecting the two asymptotic boundaries. On the right hand side, we sketch the (compact) boundary with CFT_1 and the interior of the bulk between the boundary and the bifurcation surface \mathcal{B} . This surface \mathcal{B} is also an extremal surface. \mathcal{C} and \mathcal{D} sketch typical extremal surfaces anchored to the boundary, as found in [25, 33], while \mathcal{A} depicts the possibility of an additional closed extremal surface that might appear in higher curvature theories.

boundary and thus determine the total entropy of the dual CFT. These surfaces play a role when larger regions of the boundary are considered [25].

In Einstein-Hilbert gravity, closed extremal surfaces of the area functional only exist in black hole backgrounds. They are always the bifurcation surface(s) of the black hole, at least assuming the weak energy condition: $T_{\mu\nu}V^\mu V^\nu \geq 0$ for any timelike vector V^μ (see [27, 35]). The RT prescription, being restricted to equal time slices, will then naturally equate CFT entropy with the area of the outer (if an inner one exists at all) bifurcation surface, as expected from standard AdS/CFT lore [22]. In order to reproduce this result in the HRT prescription, as mentioned in the previous section, one has to impose additional constraints such as the causality constraint [25]. The CFT entropy is then correctly determined by the (outer) bifurcation surface \mathcal{B} , and is then equal to the usual Bekenstein-Hawking black hole entropy

$$S_{BH} = \frac{\text{Area}(\mathcal{B})}{4G_N}. \quad (3.1)$$

In higher curvature theories, we may argue by symmetry that black hole bifurcation surfaces will also be saddle points of any functional of the form (2.4): The bifurcation surface is defined by the vanishing of a Killing vector field ξ . By symmetry the functional, when evaluated on certain curves, has to be invariant under flows generated by this Killing field. Hence the bifurcation surface will define a saddle point of this functional in spacetimes with the typical global structure of a black hole, see figure 3. It is an important consistency check that when evaluated on the (outer) bifurcation surface of a black hole, the functional (2.4) reproduces Wald's formula [18–20] for black hole entropy in higher curvature theories. However, due to the complexity of the functional (2.4) compared to the area functional of Einstein-Hilbert gravity, it is possible for other closed extremal surfaces to exist, even

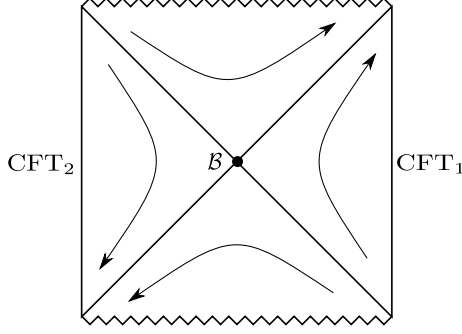


Figure 3. Conformal diagram of a static asymptotically AdS black hole. The bifurcation surface is denoted by \mathcal{B} , the singularities are drawn as zig-zag lines, the event horizons are the black diagonals and the timelike Killing vector field ξ is denoted by the arrows.

in non-black hole backgrounds. For a black hole geometry, this is sketched in figure 2. A priori it is not clear in this case whether the RT-like and HRT-like prescriptions will both correctly identify the (outer) bifurcation surface as the closed extremal curve associated to total CFT entropy. This is addressed in section 6, after investigating the existence of such surfaces in NMG and 4+1-dimensional Gauss-Bonnet gravity in the following sections.

4 Extremal curves in New Massive gravity

4.1 NMG and proposed entropy functional

The action for New Massive gravity (NMG) with cosmological parameter λ in its Lorentzian form is given by [29, 30]

$$S = \frac{1}{16\pi G_N} \int d^3x \sqrt{-g} \left[\sigma R - 2\lambda m^2 + \frac{1}{m^2} \left(R_{\mu\nu} R^{\mu\nu} - \frac{3}{8} R^2 \right) \right], \quad (4.1)$$

where the mass parameter m^2 can take any sign, and $\sigma = \pm 1$ is the sign of the Einstein-Hilbert term. This theory has been investigated in a holographic context for example in [36–43]. For later convenience, some important properties of this theory are detailed in the following [30]:

For $\lambda \geq -1$ the equations of motion from the above action admit maximally symmetric vacua as solutions. In particular, NMG admits AdS_3 vacua with the AdS radius ℓ (and $\Lambda = -1/\ell^2$) determined by the real solutions of the equation

$$\frac{1}{\ell^2} = 2m^2 \left(\sigma \pm \sqrt{1 + \lambda} \right). \quad (4.2)$$

When linearising around a maximally symmetric background with curvature Λ , negative energy gravitons (ghosts) are avoided when

$$m^2(\Lambda - 2m^2\sigma) > 0, \quad (4.3)$$

while the Breitenlohner-Freedman (BF) bound reads

$$-2m^2\sigma \geq \Lambda. \quad (4.4)$$

By using the Brown-Henneaux reasoning [44] on higher curvature theories, the central charges of the dual CFT of NMG have been determined to be [30, 45]

$$c = \frac{3\ell}{2G_N} \left(\sigma + \frac{1}{2m^2\ell^2} \right), \quad (4.5)$$

implying a clash between unitarity and positive energy in the bulk, and positive central charge of the boundary CFT: the ghost-free condition (4.3) and the condition $c \geq 0$ are mutually exclusive. Amongst other solutions, NMG gravity admits the BTZ black hole [46, 47], whose entropy is proportional to the above central charge [30, 45]:

$$\mathcal{S}_{BTZ} = \frac{2\pi r_+}{4G_N} \left(\sigma + \frac{1}{2m^2\ell^2} \right). \quad (4.6)$$

r_+ is the radius of the (outer) event horizon. Positivity of the BTZ black hole entropy hence demands the positivity of the central charge.

For NMG, the functional (2.4) for the holographic calculation of entanglement entropy reduces to [48]

$$\mathcal{S}_{EE} = \frac{1}{4G_N} \int d\tau \sqrt{g_{\tau\tau}} \left[\sigma + \frac{1}{m^2} \left(R_{||} - \frac{1}{2}k^2 - \frac{3}{4}R \right) \right], \quad (4.7)$$

whose evaluation on a particular extremal surface (or curve, since we are in 2+1 dimensions) is proposed to compute entanglement entropy in the dual boundary theory. The integral is performed along a curve parametrised by τ , with the induced metric $\sqrt{g_{\tau\tau}} = \sqrt{g_{\mu\nu} \frac{dx^\mu}{d\tau} \frac{dx^\nu}{d\tau}}$. In Einstein-Hilbert gravity, the entropy functional in 2+1 dimensions just computes the length of a path, and its extremisation produces the geodesic equations of motion. However in NMG, the evaluation of functional (4.7) no longer has the interpretation of length, due to the presence of additional curvature terms.

In the following we investigate the nature of the extremal curves corresponding to (4.7) in (partially) static backgrounds by deriving and solving the equations of motion. In the light of section 3 we pay particular attention to closed extremal curves.

4.2 Equations of motion of NMG entropy functional

As we mentioned in section 2, in using the functionals (2.4) to calculate entanglement entropy holographically, first the correct co-dimension two surface upon which the functional is evaluated needs to be found. It is hoped that one way of locating these surfaces is by directly extremising the functionals [16], and in light of this we investigate the possible curves which extremise (4.7), considering global AdS_3 and non-rotating BTZ black hole backgrounds. In 2+1 dimensions, these metrics take the form:

$$ds^2 = - \left(-M + \frac{r^2}{\ell^2} \right) dt^2 + \left(-M + \frac{r^2}{\ell^2} \right)^{-1} dr^2 + r^2 d\phi^2 \quad (4.8)$$

in Schwarzschild coordinates. The global AdS_3 metric is obtained by setting the BTZ black hole mass $M = -1$. We obtain the curves which extremise (4.7) as follows:

By considering curves that lie in a constant time slice of $t = 0$,³ we may choose the parameterisation $r = f(\phi)$, i.e. the progression of the curve into the bulk spacetime is given as a function of the (boundary) coordinate ϕ . This can be inserted into (4.7), giving

$$\mathcal{S}_{EE} = \frac{1}{4G_N} \int d\phi \, \sigma \left(f(\phi)^2 + \frac{f'(\phi)^2}{\frac{f(\phi)^2}{\ell^2} - M} \right)^{\frac{1}{2}} \left(1 + \frac{1 - \ell^2 k^2(\phi)}{2\sigma m^2 \ell^2} \right) \quad (4.9)$$

with the extrinsic curvature term

$$k^2(\phi) = -\frac{1}{\ell^2 \left(M\ell^2 f(\phi)^2 - f(\phi)^4 - \ell^2 f'(\phi)^2 \right)^3} \left(-2M\ell^2 f(\phi)^4 + f(\phi)^6 \right. \\ \left. - 2M\ell^4 f'(\phi)^2 + f(\phi)^2 \left(M^2 \ell^4 + 3\ell^2 f'(\phi)^2 \right) + M\ell^4 f(\phi) f''(\phi) - \ell^2 f(\phi)^3 f''(\phi) \right)^2.$$

The corresponding fourth order Euler-Lagrange equation of motion for $f(\phi)$ is quite involved, and we relegate the explicit expression to equation (B.3) of appendix B.

In following we discuss this equation and its possible solutions, which was in part already done in [42]. We begin with solutions anchored to the boundary.

4.3 Curves anchored at the boundary

The fourth order nature of equation (B.3) arises from the presence of the extrinsic curvature term k^2 in (4.7), and therefore to find a unique solution when solving this equation we have to specify initial conditions up to third order in derivatives, i.e. values $f(\phi_0), f'(\phi_0), f''(\phi_0), f'''(\phi_0)$. However it is first interesting to note that the geodesics of background (4.8), which are used to calculate entanglement entropy holographically in Einstein-Hilbert gravity, solve (B.3) independently of the NMG m^2 parameter⁴. For global AdS₃ this was already noted in [42]. Setting $\ell = 1$, these geodesics are [25, 33]

$$f(\phi) = \frac{\cos(\phi_0)}{\sqrt{\cos(\phi)^2 - \cos(\phi_0)^2}} \quad (4.10)$$

for global AdS₃, and

$$f(\phi) = r_+ \left(1 - \frac{\cosh^2(r_+ \phi)}{\cosh^2(r_+ \phi_0)} \right)^{-\frac{1}{2}} \quad (4.11)$$

for a non-rotating BTZ background, with event horizon radius $r_+ = \sqrt{M}$.

Other solutions can be found numerically, solving for curves with a turning point $f'(\phi_0) = 0$ at some initial radius $f(\phi_0)$ in the bulk. This allows us by symmetry to set $f'''(\phi_0) = 0$, leaving the freedom to specify $f''(\phi_0)$. In global AdS₃, we find non-geodesic curves anchored

³This can be assumed as the vector ∂_t is a Killing vector in all the spacetimes we will work with.

⁴This is likely a consequence of the fact that an interval is merely the 1-ball. In [49] an argument was presented that when the boundary region is a ball, the corresponding holographic entangling surface in AdS space can be found by an argument using topological black holes, and is independent of the bulk gravity theory.

to the boundary when the collective NMG parameter $\sigma\ell^2m^2$ is negative. In fact, for a given finite interval A on the boundary, for this parameter range there seems to exist an infinite number of different curves attached to ∂A . For the non-rotating BTZ black hole background, we again appear to find an infinite number of curves anchored to a given boundary region for $\sigma\ell^2m^2 > 0$, figure (4).

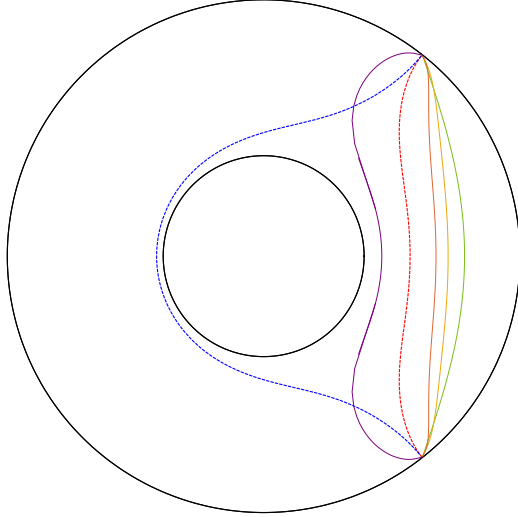


Figure 4. Diagram of a spacelike slice of the spacetime (4.8) for the choice of parameters $\sigma = \ell = 1, M = 1/2, m^2 = 1/4$. The outer (black) circle is asymptotic infinity, mapped to a finite radius via $r \rightarrow \arctan(r)$. The inner (black) circle is the bifurcation surface, the additional closed extremal curve in the bulk is not shown. The two dashed curves are geodesics (4.11) and hence solutions of (B.3) that are independent of m^2 , see text. The other curves depicted are some of the other non-geodesic solutions to (B.3), anchored to the same boundary points.

The freedom to specify an initial condition on $f''(\phi_0)$ in the above appears to be behind the emergence of the multiplicity of extremal curves associated to a given boundary interval. Notably, there also appears to be an infinite subset of these curves which satisfy the homology constraint. Given the higher derivative nature of the equations (B.3), it is likely that a sufficient set of boundary conditions would select the appropriate curve for entanglement entropy. We leave the investigation of correct boundary conditions on these holographic entangling curves for future research, as it is beyond the scope of our paper. In any case, in section 6 we will present another consistency argument that also constrains this infinite set of curves in such a way that only the geodesic solutions remain.

In the next section we will consider the possible closed extremal curves, which we are to study analytically. The corresponding value of entropy can then be easily calculated as no boundary terms are required.

4.4 Closed extremal curves in NMG

For the study of closed extremal curves, to begin we restrict our attention to black hole backgrounds. In particular, for this section we focus on the non-rotating BTZ black hole while in appendix C we comment on the rotating case, and Lifshitz black holes. In section

3 the significance of closed extremal curves of holographic entropy functionals in black hole backgrounds was explained.

While the Schwarzschild coordinates (4.8) do not cover the BTZ black hole event horizon, following the discussion of section 3 the BTZ black hole bifurcation surface $r_+ = \ell\sqrt{M}$ is a closed extremal surface of entropy functional (4.7). The corresponding value of the entropy functional is equal to the entropy of the black hole (4.6):

$$\mathcal{S}_{EE+} = \mathcal{S}_{BTZ} = \frac{2\pi\ell\sqrt{M}}{4G_N} \left(\sigma + \frac{1}{2\ell^2 m^2} \right). \quad (4.12)$$

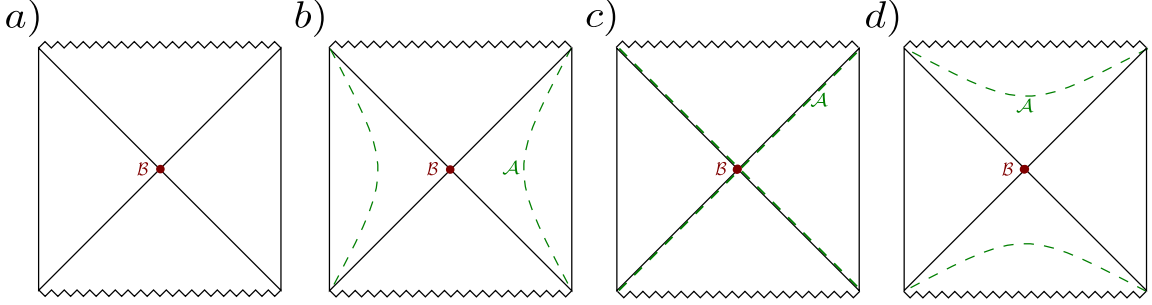


Figure 5. *a)*: Conformal diagram of the BTZ black hole (4.8) without additional extremal surfaces as also in figure 3. The bifurcation surface is denoted by \mathcal{B} , the singularities are drawn as zig-zag lines and the event horizons are the black diagonals. The appearance of additional closed extremal surfaces [*b*] – [*d*]] is not entirely a feature of the geometry (as geodesics would be), but also depends on the parameters of the gravitational theory. Additional extremal surfaces (\mathcal{A}) can be outside of the event horizon [*b*]], inside of it [*d*]] or in special cases they can coincide with slices of the event horizon [*c*]].

To find closed curve solutions to the equation of motion (B.3), we set $f' = f'' = f''' = f'''' = 0$. For the same range that the multiplicity of extremal curves anchored to the boundary appears in the non-rotating BTZ background ($\sigma\ell^2 m^2 > 0$), we find an additional closed extremal curve located at radial distance⁵

$$r_a = \sqrt{\frac{M}{2\sigma m^2}} \quad (4.13)$$

from the centre. Notice that $r_a \geq r_+$ is equivalent to the BF bound (4.4). Our results for these additional closed bulk extremal curves are summarised in figures 5 and 6. The value of the entropy functional corresponding to r_a is

$$\mathcal{S}_{EEa} = \frac{2\pi\sigma}{4G_N} \sqrt{\frac{2M}{\sigma m^2}}. \quad (4.14)$$

Comparing this value with the entropy of the BTZ black hole \mathcal{S}_{BTZ} , we find $|\mathcal{S}_{BTZ}| \geq |\mathcal{S}_{EEa}|$ with equality for $\sigma\ell^2 m^2 = 1/2$ where $r_a = r_+$, i.e. where the BF bound is saturated. For

⁵Performing the same calculation in Kruskal coordinates, one can show that this also holds when the additional closed extremal curves are inside the event horizon.

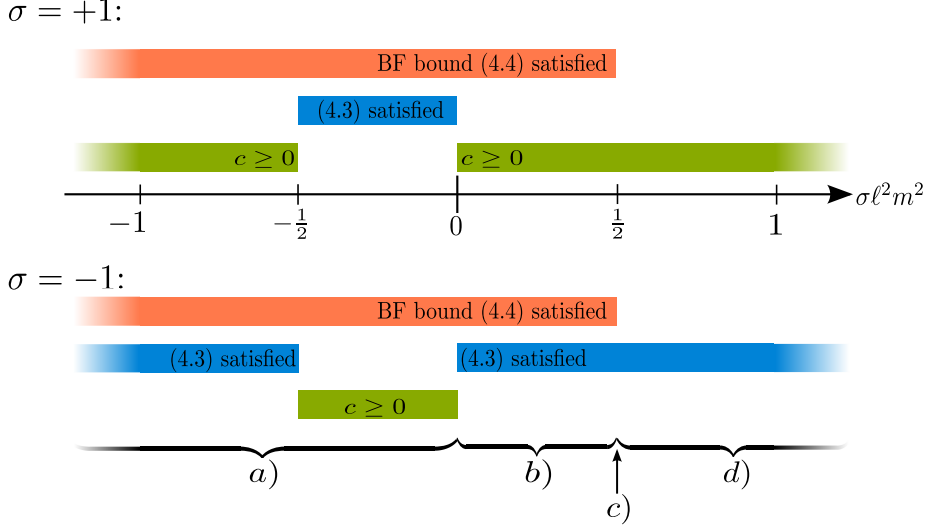


Figure 6. An overview over the parameter-space of NMG: For the two possible choices $\sigma = +1$ and $\sigma = -1$, it is depicted for which values of $\sigma \ell^2 m^2$ the inequalities (4.3) and (4.4) are satisfied and (4.5) yields positive central charges. Comparing (4.13) and $r_+ = \ell \sqrt{M}$, we can depict for which value of $\sigma \ell^2 m^2$ what type of additional extremal surface (see $a) - d)$ in figure 5) appears.

positive central charges (and hence positive BTZ entropy), the additional extremal surfaces will correspond to a lower entropy than the Wald entropy of the black hole. Hence in both RT- and HRT-like prescriptions, naively invoking only the homology constraint and that the entropy is minimised would lead one to incorrectly identify \mathcal{S}_{EEa} with the entropy of the dual CFT for certain choices of $\sigma \ell^2 m^2$. We elaborate on how this changes in the HRT-like prescription when causality constraints are imposed in section 6.

The existence of additional closed extremal curves is not restricted to the non-rotating BTZ background: they also exist for the rotating BTZ and Lifshitz black hole backgrounds, see appendix C.

As a further simple example let us consider global AdS spacetime, which can be obtained by setting $M = -1$ in the BTZ metric (4.8). It follows from equations (4.13) and (4.14) that we also get additional closed extremal curves in the bulk of AdS for $\sigma \ell^2 m^2 < 0$, which is case $a)$ in figure 6. The corresponding entropy will be positive for $\sigma = +1$ and negative for $\sigma = -1$. In the case of negative entropy, these additional curves hence correspond to an entropy lower than the value which is physically expected. As in the above, we would be led to incorrectly identify this with the CFT entropy. It can be seen from figure 6 that part of this parameter range (for example $\sigma = -1$ and $\sigma \ell^2 m^2 < -1/2$) is free of ghosts, but the central charge of the dual theory would be negative. We will return to the issue of closed extremal curves in an AdS bulk spacetime in section 5. In section 6 we will also explain how the causality argument can be employed to rule out these additional curves.

As NMG is afflicted with problems regarding ghosts in the bulk (violation of inequality (4.3)), one might ascribe the additional closed curves we find in the theory to instabilities of the background. However, the parameter ranges in which the additional curves exist and that in which ghosts appear are not in one-to-one correspondence (see figure 6). For

example, global AdS space can have additional closed curves without ghosts, while for the BTZ black hole at $\sigma = +1$, $\sigma\ell^2 m^2 = -1$ the theory exhibits ghosts and does not show additional extremal curves. There is therefore no obvious and transparent connection between the appearance of ghosts and the additional curves.

In the following section, as another example we consider the existence of additional closed extremal surfaces in Gauss Bonnet gravity.

5 Closed extremal surfaces in Gauss-Bonnet gravity

Gauss-Bonnet gravity

Gauss-Bonnet gravity is a special case of Lovelock gravity [31] (see [32] for a review) and has been extensively studied before in the holographic context, see for example [21, 50] and [51, 52] for reviews. For simplicity we will restrict our discussion to five bulk dimensions, in which the (Lorentzian) action reads

$$S = \frac{1}{16\pi G_N} \int d^5x \sqrt{-g} \left[R + \frac{12}{L^2} + \lambda \frac{L^2}{2} \left(R_{\mu\nu\alpha\beta} R^{\mu\nu\alpha\beta} - 4R_{\mu\nu} R^{\mu\nu} + R^2 \right) \right] \quad (5.1)$$

adopting the conventions used for example in [50]. The conjectured boundary theory is causal for [53–56]⁶

$$-\frac{7}{36} \leq \lambda \leq \frac{9}{100}, \quad (5.2)$$

and it is possible to choose an AdS vacuum such that the bulk theory is ghost free [57] and the dual CFT is unitary (see e.g. [51, 52]). The entropy functional (2.4) takes the form

$$\mathcal{S}_{EE} = \frac{1}{4G_N} \int_{\Sigma} d^3y \sqrt{\gamma} \left(1 + \lambda L^2 \mathcal{R} \right), \quad (5.3)$$

where the Gauss-Codazzi equations have been used to absorb the extrinsic curvature terms into the intrinsic scalar curvature \mathcal{R} of Σ . This functional, known as Jacobson-Myers functional, has already been derived in [58] in the context of black hole entropy. It was later proposed for the holographic calculation of entanglement entropy in [14, 21, 24, 50].

Closed extremal surfaces

At the level of the entropy functional it is possible to conclude that spherically symmetric spacetimes in Gauss-Bonnet gravity also admit additional closed extremal surfaces: Suppose we are working with a stationary spherically symmetric black hole background of Gauss-Bonnet gravity (see e.g [59–62]), given in Schwarzschild-like coordinates t, r, θ, ϕ, ψ . Similar to section 4.4, we assume that the spacelike surface Σ is adopted from the spherical symmetry of the spacetime, i.e. that Σ is a 3-sphere parametrized by $t = \text{const.}$, $r = \text{const.}$,

⁶ Similar conditions on the value of λ have been derived in [23] by demanding positivity of holographic relative entropy.

with θ, ϕ, ψ arbitrary. It then follows that $\int_{\Sigma} \sqrt{\gamma} = \text{Area}(\Sigma) = 2\pi^2 r^3$ and $\mathcal{R} = 6/r^2$, such that the functional (5.3) takes the form

$$\mathcal{S}_{EE} = \frac{\pi^2}{2G_N} (r^3 + 6\lambda L^2 r). \quad (5.4)$$

For negative λ this has a minimum at finite $r = \sqrt{-2\lambda}L$, implying the existence of a closed extremal surface at this radius.⁷⁸ From a similar calculation as above, we see that for $\lambda > 0$ additional extremal surfaces appear in hyperbolic backgrounds (where $\mathcal{R} < 0$) at a radius $r = \sqrt{2\lambda}L$. We now consider these additional extremal surfaces in a few simple backgrounds.

AdS and boson stars

For spherically symmetric spacetimes such as global AdS or boson stars [64, 65],⁹ the additional surfaces are problematic. In these cases the additional surface would be competing with the empty surface, which corresponds to zero entropy. As the additional surface found above corresponds to negative entropy, naively following the prescription to take the surface extremising the functional with lowest entropy as the entangling surface would lead to erroneously prescribing a negative entropy to the CFT duals of AdS space and boson stars. Yet, as will be shown in section 6 the causality argument presented will be sufficient to exclude these surfaces, so that the entropy of the CFT dual to an AdS or boson star spacetime is correctly identified as zero.

Black holes

Note that the above argument for closed extremal surfaces is independent of the topology of the bulk spacetime, therefore in a stationary black hole spacetime, in addition to the surface found above, the black hole bifurcation surface would also be a closed extremal surface. For ghost free black hole backgrounds, the additional closed surface we find is not necessarily an issue due to the existence of lower bounds on the horizon radius which are larger than the radius of the additional surface. For the case of vacuum black holes [61, 62] and charged hyperbolic black holes [63], this bound on the event horizon exactly coincides with the radius of the additional surface. This means that these additional surfaces can never be outside of the event horizon, in the static region of the bulk spacetime. These black hole solutions can also have curvature singularities at finite radial coordinate. In the vacuum case [61, 62], this singularity is located at a larger value of the radial coordinate than the additional surface, the latter one hence does not appear in the spacetime at all.

⁷ It was recently shown [48, 67–69], that the equations of motion originating from functionals that depend only on intrinsic curvature terms (such as (5.3)), take the general form $X^{ij} k_{ij}^{(\alpha)} = 0$, where $k_{ij}^{(\alpha)}$ describes the extrinsic curvature projected onto Σ . For Gauss-Bonnet gravity, we have $X^{ij} = \frac{1}{2}\gamma^{ij} + \lambda L^2 (\frac{1}{2}\gamma^{ij}\mathcal{R} - \mathcal{R}^{ij})$. It is then easy to show that the additional closed bulk extremal surface at $r = \sqrt{-2\lambda}L$ exactly solves these equations of motion with $X^{ij} = 0$. See also section 7 for a discussion of these equations in the context of the alternative conical boundary condition method.

⁸The case $\lambda < 0$ is less studied, for in the context of string-theory one is restricted to $\lambda > 0$ [57].

⁹Although the given sources only investigate boson stars for $\lambda > 0$, we were assured by Betti Hartmann and Yves Brihaye that similar solutions can also be found for $\lambda < 0$.

For the charged solutions [63] in contrast, the singularity can be located at a sufficiently low value of the radial coordinate such that the additional extremal surfaces appear at least inside of the outer event horizon, as in figure 5d). As the region inside the black hole is not static, this would be a problem in the HRT-like prescription.

6 Closed bulk extremal surfaces and the causal influence argument

In this section, we will present an argument based on causality that can be employed in Lorentzian settings to consistently eliminate the additional extremal surfaces found to be problematic throughout this paper.

The causal influence argument

We first explain that the presence of the additional closed extremal surfaces found in this paper indicates a subtle difference between RT- and HRT-like prescriptions, when causality conditions are taken into account.¹⁰ More specifically, we will show that in HRT-like prescriptions, an argument based on causality can be used to argue that these surfaces cannot be used to calculate entanglement entropy.

In section 2 we explained how the area functional can be employed to calculate holographic entanglement entropy in Einstein-Hilbert gravity, with subtle differences between the RT and HRT prescriptions that could be resolved by imposing causality conditions on the latter, see also [25, 27]. Spacetimes for which such differences were found in [25] are the Reissner-Nordström black hole and the bag-of-gold spacetime, where an eternal black hole is matched to a compact spacetime bubble along a static shell of matter [70, 71].

As was furthermore explained in section 2, for higher curvature theories such as (2.3), functionals (2.4) generalising the area functional have been proposed to calculate entanglement entropy holographically. As these functionals were derived in Euclidean settings in [14–17], a priori these functionals should be seen to be most reliable in an RT-like setting. However, as all the spacetime backgrounds that are considered in the present work are at least partially (i.e. not necessarily globally) static, one would naively expect RT- and HRT-like prescription in using these functionals to agree. Here we will now consider how the imposition of a causality argument due to Headrick, Hubeny, Lawrence and Rangamani [27, 28], which we refer to as the *causal influence argument*, affects this expectation in our cases:

The principle behind the causal influence argument is to avoid causality paradoxes similar to the well known grandfather paradox. Suppose one wanted to calculate the entanglement entropy of a certain boundary region A (at boundary time $t = 0$) using a bulk co-dimension two surface \mathcal{E}_A . If \mathcal{E}_A were to lie in the future of A , i.e. that there were to be a future pointing timelike curve from A to (at least one point on) \mathcal{E}_A , the following paradox might arise: An observer living on (or near) the boundary might immediately after $t = 0$ send some energy into the bulk in such a way that the geometry around the part of \mathcal{E}_A in the future of A is changed. This would also affect the surface \mathcal{E}_A itself, hence potentially

¹⁰As explained before, following [16], in the RT- and HRT-like prescriptions we adopt the method of locating the entangling surface which involves extremising the entropy functionals.

the associated entropy. This has the implication that it would be possible — after the entanglement entropy was fixed from the point of view of the CFT — to alter the result of the holographic entanglement entropy calculation in the bulk, leading to an obvious paradox. We therefore demand that there should be no timelike curve from A to \mathcal{E}_A , and by time inversion symmetry also not from \mathcal{E}_A to A . Similarly, the same holds for \mathcal{E}_A and \bar{A} , the complement of A . Hence, causality implies that \mathcal{E}_A should be required to lie in the *causal shadows* of the boundary regions A and \bar{A} , i.e. there should be no timelike curves connecting \mathcal{E}_A to one of the two regions¹¹. For reasons that will soon become clear, we refer to this as the *weak form* of the causal influence argument. The explanation presented here may of course be at most a motivation and not a stringent derivation of the necessity to impose this causality condition on the extremal surfaces, however we will find this condition to be very useful in the discussion below.

This condition can still be strengthened, and to explain how let us describe the way in which this argument comes into play in RT- and HRT-like prescriptions. As explained in section 2, the RT-like prescription assumes a static bulk spacetime, in which due to the presence of a timelike Killing vector field one can unambiguously define a foliation of the bulk spacetime (as well as of the conformal boundary) into spacelike slices. Both the boundary region A and the co-dimension two surface \mathcal{E}_A are then embedded in one of these spacelike slices by construction and the weak form of the causal influence argument is therefore trivially satisfied, see the left side of figure 7.

On the other hand, the HRT prescription is intended to work for general spacetimes, and therefore the existence of a uniquely defined foliation of the bulk spacetime cannot be assumed. Similarly, the boundary region A on the conformal boundary does not need to lie on an equal time slice of the boundary time. As long as the boundary ∂A (to which \mathcal{E}_A will be anchored) is held fixed, the entanglement entropy of A , and \mathcal{E}_A , are supposed to be independent of deformations of A within its domain of dependence \diamond_A , see figure 8. The *domain of dependence* \diamond_A is defined as the set of all points on the boundary where every causal curve going through one of these points necessarily intersects A . Due to the possibility of deforming A in the HRT prescription, the causal influence argument can be formulated in what we refer to as its *strong form*:

\mathcal{E}_A should be required to lie in the causal shadows of any possible spacelike deformations ($A', \bar{A}', A'', \bar{A}'' \dots$) of both A and \bar{A} leaving the boundaries ∂A and $\partial \bar{A}$ invariant.

or equivalently

\mathcal{E}_A should be required to lie in the causal shadows of the interiors of both \diamond_A and $\diamond_{\bar{A}}$.

See also the right of figure 7 for an illustration.

¹¹A note on nomenclature: The *causal shadow* of a certain spacetime as originally defined by Headrick, Hubeny, Lawrence and Rangamani [27] is supposed to be the set of points in the bulk which are not causally connected to any point in the boundary, irrespective of any division of the boundary into subsystems A and \bar{A} . Here we use this term also to define regions of the bulk which are not in causal contact with specific subregions of the boundary.

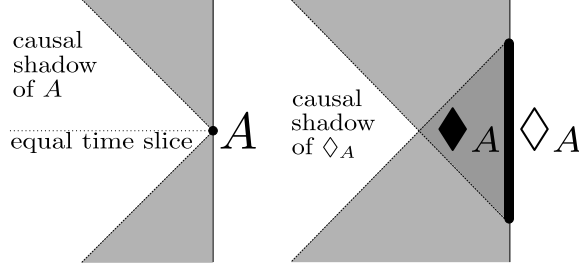


Figure 7. In an RT-like prescription (left), the boundary region A is restricted to lie on an equal time slice of the boundary, uniquely defined by a fixed value of the Killing time coordinate t . The holographic entangling surface belonging to A lies by construction on a similarly defined equal time slice of the bulk spacetime, and hence in the causal shadow of A . The weak form of the causal influence argument is hence satisfied by construction. In an HRT-like prescription (right), A can be deformed within its domain of dependence \diamond_A as shown in figure 8. The holographic entangling surface then has to be in the causal shadow of \diamond_A . Even for a partially static spacetime where RT and HRT are expected to be equivalent, this strong form of the causal influence argument is a severe restriction, as the part of the equal time slice inside of \blacklozenge_A would also be excluded by this argument. The region \blacklozenge_A in which signals can be both send to and received from \diamond_A is called the *causal wedge*, see [72]. The complement \bar{A} of A and its domain of dependence $\diamond_{\bar{A}}$ cause a similar causal shadow that extends into the bulk.

It is very interesting to note that although RT- and HRT-like prescriptions are expected to agree on static spacetimes, the strong form of the causal influence argument is nontrivial in a static spacetime: It excludes a part of the spacelike slice on which \mathcal{E}_A would be located by construction in the RT-like prescription, and which in the RT-like prescription would not be excluded by any simple and obvious conditions. This means that the strong form of the causal influence argument points out a far from trivial difference between RT-like prescriptions and HRT-like prescriptions amended with a causality argument¹² in general gravitational theories of the form (2.3). For Einstein-Hilbert gravity it has been proven in [26, 33, 72] that holographic entangling surfaces anchored at the boundary can never enter the causal wedge of the corresponding boundary region.¹³ So this implies that if the strong form of the causality condition is satisfied in a HRT-like prescription, and if the HRT-like prescription (supplemented with the causality condition) is to agree with the RT-like prescription on static spacetimes, then the latter needs to obey conditions that can be derived in the Euclidean setting and act as a precursor to the causality argument in a Lorentzian setting.

In the previous sections 4.4 and 5 we showed that functionals of the form (2.4) may in many cases allow for additional closed extremal surfaces in AdS black hole and global AdS spacetimes, see e.g. figure 5. Due to standard AdS/CFT results, these surfaces can be expected to be unphysical. In the HRT prescription, the strong form of the causal influence argument presented above can be used to rule out these additional extremal surfaces, as we

¹²Recall that for Einstein-Hilbert gravity, in [25] these causality arguments were argued to be necessary to make the RT and HRT prescriptions agree in certain cases.

¹³Furthermore, in [27] a proof of the strong form of the causal influence argument in Einstein-Hilbert gravity is presented, assuming the null energy condition and some other technical details.

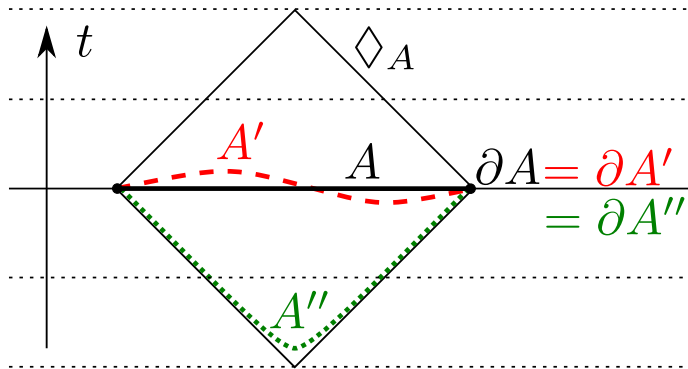


Figure 8. In an HRT-like approach to entanglement entropy, the entangling region is not necessarily fixed to an equal time ($t = \text{const.}$) slice such as A . In fact, as long as the region stays spacelike and the boundary ∂A stays fixed (and hence stays inside of the domain of dependence \diamond_A), one can deform A to take shapes such as A' and A'' in the above picture.

demonstrate in the remainder of this section.

Black hole backgrounds

In black hole spacetimes, it is clear that at least when the additional extremal surfaces are outside of the black hole event horizon (case *b*) in figure 5), for a given time slice of the bulk spacetime there will always be an additional extremal surface on this slice homologous to the full boundary. In an RT-like prescription, the conditions on the extremal surfaces¹⁴ would lead one to deduce that the additional extremal surface outside the black hole bifurcation surface determines the total entropies of CFT_1 and CFT_2 , since it gives a lower entropy. This would be a serious problem, as it would imply a mismatch between CFT and black hole entropy. Now let's look at this problem in a HRT-like (i.e. manifestly Lorentzian) framework, where causality arguments can be used. Consider the setup depicted in figure 9. If A is a complete equal time slice of the right boundary (and hence \bar{A} of the left), then \diamond_A is the complete right boundary in its full extent in space and time (and similarly $\diamond_{\bar{A}}$ is the complete left boundary). Requiring that the entangling surface(s) corresponding to this division of the total system into subsystems A and \bar{A} are not connected to any point on the boundaries via timelike curves leaves the black hole bifurcation surface as the only possible extremal surface, see figure 9. Therefore, the strong form of the causal influence argument leads (in the cases studied in this paper) to an agreement between black hole entropy and holographic CFT entropy.

Global AdS

Both for NMG (section 4.4) and Gauss-Bonnet gravity (section 5) we also found closed extremal surfaces in the bulk of global AdS spacetime. As explained in section 5, these additional extremal curves have to be compared with the empty curve, which assigns zero entropy to the dual CFT and is allowed by the homology condition in topologically trivial

¹⁴The homology condition and minimisation of the entropy.

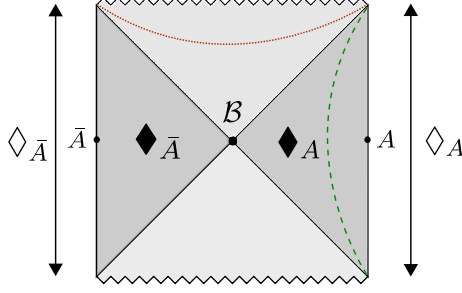


Figure 9. When the region A in the CFT is a full equal time slice of the right boundary, the causal wedges \Diamond_A and $\Diamond_{\bar{A}}$ together cover the entire region outside the event horizons of the black and white holes. As illustrated by the dashed green line, all closed extremal surfaces outside the black hole event horizon lie in this region and are thus ruled out by the strong form of the causal influence argument. The dotted red line representing an additional closed extremal surface inside the event horizon is also forbidden, as it is timelike connected to \Diamond_A and $\Diamond_{\bar{A}}$. The intersection of causal shadows of both \Diamond_A and $\Diamond_{\bar{A}}$ is therefore the bifurcation surface \mathcal{B} of the black hole (which is called the causal shadow of the spacetime), leaving it as the only permissible closed extremal surface.

spacetimes. As global AdS spacetime does not contain any event horizons, the entire bulk is in causal contact with the boundary CFT. Therefore, for the full boundary as CFT subsystem A the causal influence argument rules out any curve in the bulk, leaving only the empty curve to correctly determine the CFT entropy as zero. This argument similarly applies to any other topologically trivial spacetime, such as for example boson stars mentioned in section 5.

Curves anchored at the boundary

Let us now come to the additional extremal curves anchored at the boundary that we found in section 4.3, see especially figure 4. The calculations of that section were carried out on AdS and BTZ background spacetimes. For such background spacetimes, it is known that (on an equal time slice) the boundary of the causal wedge of a certain boundary region A will be given by a spacelike geodesic of the form (4.10) and (4.11) respectively, see [33]. We can now easily see that the additional (non-geodesic) extremal curves found in section 4.3 are ruled out by the strong form of the causal influence argument by examining figure 4. There, we see two geodesics anchored at the boundary, drawn as thick dashed (red and blue) lines. The first one (drawn in red) is similar to the curve labeled by \mathcal{C} in figure 2 and marks the boundary of the causal wedge \Diamond_A corresponding to the boundary region A . The second one (drawn in blue) is the equivalent of curve \mathcal{D} in figure 2 and marks the boundary of $\Diamond_{\bar{A}}$, the causal wedge of \bar{A} . In figure 4 it is now easy to see that the additional, non-geodesic extremal curves discussed in section 4.3 are excluded by the strong form of the causal influence argument: They either enter \Diamond_A or $\Diamond_{\bar{A}}$, and hence leave the causal shadow of either A or \bar{A} . Apart from the geodesics which are located exactly at the boundary of the causal wedges, we didn't find any additional curves which are not excluded by the strong form of the causal influence argument.

Summary

In summary, we find that for the examples of (partially) static spacetimes in NMG and Gauss-Bonnet gravity considered here, only the HRT-like prescription amended with the strong form of the causal influence argument can ensure physical results for entanglement entropy. This is in contrast to the Einstein-Hilbert case, where the RT and the HRT prescription amended with the causal influence argument agree on such spacetimes. For RT-like prescriptions, due to their manifestly Euclidean nature, it is not possible to make arguments based on causality. Nevertheless, if RT-like prescriptions and HRT-like prescriptions with causality conditions are supposed to agree on (partially) static spacetimes, the surfaces found in the RT setting need to obey the causality conditions which only make sense in a covariant framework. This implies the fascinating possibility that there exists a condition that has to be imposed in the RT-like approach in addition to the homology constraint, and which can be derived by arguments completely independent of causality. This condition would act as a precursor to the (strong form of the) causal influence argument that comes into effect in the Lorentzian setting. Perhaps a better understanding of holographic entanglement entropy would hopefully give conditions from first principles that exclude such pathological surfaces.

In the next section, we will investigate whether for Gauss-Bonnet gravity one can also derive conditions that rule out the additional closed extremal surfaces and fix the holographically computed CFT entropy to the expected physical value in the RT-like prescription. We will speculate on a possible connection between these conditions and the causality constraint in section 8.2.

7 Conical boundary condition method in Gauss-Bonnet gravity

Method

In [12], Lewkowycz and Maldacena proposed a method of calculating entanglement entropy holographically for CFT duals to Einstein-Hilbert gravity by introducing the concept of generalised gravitational entropy. This is an extension of the usual Euclidean methods for calculating black hole entropy to solutions without $U(1)$ symmetry in Euclidean time. In the present context, it is important to note that this method is applicable only to spatial regions in static spacetimes. To calculate entanglement entropy, the basic idea is to translate the replica trick into the bulk, where a co-dimension two hypersurface with conical defect is introduced. By expanding the bulk equations of motion about the conical singularity, and demanding finiteness of the energy-momentum tensor, the location of the holographic entangling surface can be determined. Thus entanglement entropy can be calculated. The details of this procedure for Einstein-Hilbert gravity were given in [12]. It was also applied to Gauss-Bonnet gravity in [48, 67, 68], and to general higher curvature theories of the form (2.3) in [16, 17].

The metric describing the conical singularity around a co-dimension two bulk surface can be written as [48]

$$ds^2 = e^{2\rho} (dq^2 + q^2 d\tau^2) + (\gamma_{ij} + q \cos(\tau) k_{(q)ij} + q \sin(\tau) k_{(\tau)ij}) dy^i dy^j + \dots \quad (7.1)$$

with

$$e^{2\rho} = q^{-2\varepsilon}. \quad (7.2)$$

Here, $i = 1, 2, \dots, d-1$ and ε is a small parameter that is later taken to zero in the replica trick. $k_{(\alpha)ij}$ ($\alpha \in \{\tau, q\}$) is the extrinsic curvature of the surface, and y^i are its induced coordinates. The conical singularity is localised along the surface at $q = 0$.

In Einstein-Hilbert gravity, by demanding that the equations of motion near the singularity are satisfied and regular, one arrives at the condition [12]

$$k_{(\alpha)} = 0, \quad (7.3)$$

i.e. the co-dimension two surface is a minimal area surface, thus proving the RT prescription. Note that this is only valid in static scenarios, and is therefore not a proof of the HRT prescription.

For 4+1-dimensional Gauss-Bonnet gravity, upon inserting the metric (7.1) the following components of the equations of motion become singular [48]:

$$qq\text{-component:} \quad -\frac{\varepsilon}{q}k - \frac{\lambda L^2 \varepsilon}{q} \left[k\mathcal{R} - 2k_{ij}\mathcal{R}^{ij} + q^{2\varepsilon} \left(-k^3 + 3kk_{ij}k^{ij} - 2k_{il}k^{lj}k_j^i \right) \right] \quad (7.4)$$

$$qi\text{-component:} \quad -\frac{2\lambda L^2 \varepsilon}{q} q^{2\varepsilon} \left[k\nabla_j k_i^j - k\nabla_i k + k_i^j \nabla_j k - k_{ij} \nabla_l k^{lj} + k_{lj} \nabla_i k^{lj} - k_{jl} \nabla^j k_i^l \right] \quad (7.5)$$

$$ij\text{-component:} \quad 4\lambda L^2 \left[\frac{\varepsilon}{q} q^{4\varepsilon} (k_{ij}k_{lm}k^{lm} - 2k_{il}k^{lm}k_{mj} + k_{il}k_j^l k - k_{lm}k^{lm}\gamma_{ij} + k_{ln}k^{nm}k_m^l \gamma_{ij}) + \frac{\varepsilon^2}{q^2} q^{4\varepsilon} (k^2 \gamma_{ij} - 2kk_{ij} - k_{lm}k^{lm}\gamma_{ij} + 2k_{il}k_j^l) \right]. \quad (7.6)$$

$i, j \in \{1, 2, 3\}$ are the indices of the induced metric on the co-dimension two surface, with intrinsic Ricci tensor \mathcal{R}_{ij} and $k = \text{Tr } k_{ij}$. In the above equation, there is only one extrinsic curvature k_{ij} as we are assuming a static background spacetime. In such a background, the two extrinsic curvatures of a surface on an equal time slice are always linear combinations of only one tensor k_{ij} , independently of the choice of normal coordinates. By demanding that the singular components vanish, constraints on the entangling surfaces in 4+1-dimensional Gauss-Bonnet gravity can be derived. We utilise these constraints in the following to investigate whether the closed extremal surfaces of the Gauss-Bonnet entropy functional (5.3) are valid in the holographic calculation of entanglement entropy.

Investigating conditions on closed bulk surfaces

As shown in section 5, assuming spherical symmetry the hypersphere of radius $r = \sqrt{-2\lambda}L$ on a constant time slice $t = \text{const.}$ is a closed extremal surface of the Gauss-Bonnet entropy functional (5.3) regardless of the topology of the bulk spacetime. That is, it is an extremal surface for a static spherically symmetric background of the form

$$ds^2 = -h(r)dt^2 + f(r)dr^2 + r^2\gamma_{ij}dx^i dx^j, \quad (7.7)$$

with the line element of the hypersphere

$$\gamma_{ij}dx^i dx^j = d\theta^2 + \sin(\theta)^2 d\phi^2 + \sin(\theta)^2 \sin(\phi)^2 d\psi^2, \quad (7.8)$$

independently of functions $f(r)$ and $h(r)$ in (7.7). For a static black hole spacetime, the black hole bifurcation surface is also an extremal surface of the functional.

To subject these extremal surfaces to the constraints arising from the equations of motion (7.4)–(7.6), the corresponding extrinsic curvatures need to be calculated. For a given co-dimension two surface characterised by embedding functions $x^\mu = X^\mu(y)$, the extrinsic curvature can be calculated via [68]¹⁵

$$k_{ij}^{(\alpha)} = -(n_{(\alpha)})_\mu (\nabla_i \partial_j X^\mu + \Gamma_{\rho\sigma}^\mu \partial_i X^\rho \partial_j X^\sigma). \quad (7.9)$$

Here, $\mu, \rho, \sigma \in \{0, \dots, 4\}$ are indices of the full spacetime with Christoffel symbols $\Gamma_{\rho\sigma}^\mu$, $i, j \in \{1, 2, 3\}$ are indices of the induced metric on the co-dimension two entangling surface and $\alpha \in \{1, 2\}$ labels the two orthonormal vectors $(n_{(\alpha)})^\mu$ to this surface, see also appendix A.

For the extremal hyperspheres, we will use coordinates θ, ϕ, ψ , in which terms of the form $\partial_i X^\mu$ become Kronecker-deltas. By symmetry, the extrinsic curvature $k_{ij}^{(1)}$ with respect to the normal vector $n_{(1)} = \partial_t$ will vanish identically, so we are left with

$$k_{mn} \equiv k_{mn}^{(2)} = -\sqrt{|f(r)|} \Gamma_{mn}^r = \frac{r}{\sqrt{|f(r)|}} \gamma_{mn}, \quad (7.10)$$

where by slight abuse of notation we introduced “shifted indices” $m, n \in \{\theta, \phi, \psi\}$ ¹⁶. The singular equations of motion (7.4)–(7.6) simplify greatly upon insertion of (7.10): The qi -component vanishes trivially as it only contains covariant derivatives ∇ with respect to the induced metric γ_{ij} and $k_{ij} = \text{const.}(r) \cdot \gamma_{ij}$. Using that for the hyperspheres $\mathcal{R}_{ij} = \gamma_{ij} \mathcal{R}/3$ and $\mathcal{R} = 6/r^2$, the qq -component simplifies to

$$-\frac{\epsilon}{q} \left[k \left(1 + \frac{2\lambda L^2}{r^2} \right) - \lambda L^2 \frac{2}{9} q^{2\epsilon} k^3 \right]. \quad (7.11)$$

Similarly, the ij -component reads

$$4\lambda L^2 \gamma_{ij} \left[\frac{\epsilon}{q} q^{4\epsilon} k^3 \frac{-2}{27} + \frac{\epsilon^2}{q^2} q^{4\epsilon} k^2 \frac{2}{9} \right]. \quad (7.12)$$

Testing the conditions

It is clear that a bifurcation surface, which necessarily is a geometrical extremal surface with $k = 0$,¹⁷ makes both (7.11) and (7.12) vanish identically. Additionally, we see that the

¹⁵In contrast to the quantity $k_{\mu\nu}^{(\alpha)}$ presented in appendix A where μ, ν were indices of the full spacetime, this quantity is the extrinsic curvature projected to the internal space of the hypersurface.

¹⁶We refer to these as shifted because in the latin indices the θ -component corresponds to $i = 1$, while in the greek indices the same component corresponds to $\mu = 2$. So in the usual notation the above equation would imply $k_{11} \sim \Gamma_{22}^1$ etc.

¹⁷We expect (7.7) to have an event horizon where $h(r) = 0 = 1/f(r)$, see [73] for a further discussion. It would then follow from (7.10) that $k = 0$ at the bifurcation surface.

leading divergence in (7.11) vanishes when the functional (5.4) is extremised, i.e. for any extremal curve of the functional (5.3). Hence the bifurcation surface of a black hole will always satisfy these conditions.

Let us now turn to the additional extremal surface that appears for example in global AdS space at radius $r = \sqrt{-2\lambda}L$. With extrinsic curvature (7.10), the remaining terms in (7.11), and (7.12) do not vanish. It was exactly the vanishing of this leading divergence in the qq -component that was shown in [16] to be equivalent to the equations of motion derived from extremising the proposed entropy functional. Nevertheless, it is apparent from the above computations that the other components (and perhaps the less divergent terms) may in principle contain vital information that is needed to rule out the unphysical extremal surfaces that one finds by varying the entropy functional. As (7.5) and (7.6) are proportional to λ , it is immediately apparent that these components do not play any role in Einstein-Hilbert gravity ($\lambda = 0$).

Thus, at least for the closed extremal curves in Gauss-Bonnet gravity, the conditions derived from the conical boundary condition method yield a restriction on the RT-like prescription that ensures physicality of the resulting entropy. As explained in section 6, such conditions are needed in order to play the role in the RT-like prescription that the causal influence argument plays in the HRT-like prescriptions. We would however like to add that although the conditions (7.11) and (7.12) are successful in ruling out the additional closed extremal curves in the RT-like prescription, there are cases when these constraints prove to be too restrictive. For example, it was shown in [67] that the extremal surfaces of the entropy functional corresponding to cylindrical boundary regions fail to satisfy the conditions coming from the subleading divergent component (7.4) near their turning point in the bulk.¹⁸ The conditions we have discussed in this section are therefore not yet complete for the RT-like prescription. Further investigation in this direction is worthwhile, as it seems to be a promising approach towards ruling out the additional curves in a Euclidean setting.

It is interesting to note that similar conditions on the entangling surfaces in static settings can be derived independent of the conical boundary condition method (i.e. the replica trick), by considering the Brown-York stress tensor T computed on a static co-dimension one hypersurface extending into the bulk [67, 74]. The profile of this hypersurface that defines the extension of it into the bulk is then a spacelike co-dimension two hypersurface located on an equal time slice, just as in the calculation of entanglement entropy. Indeed, for Einstein-Hilbert gravity, demanding $T_{tt} = 0$ results in a minimal surface condition on the profile of the hypersurface, in agreement with the RT prescription [74]. This seems to imply a connection between entanglement entropy and the Brown-York stress tensor. In [67] the same approach was investigated for Gauss-Bonnet gravity, and it was shown that demanding $T_{tt} = 0$ imposes the following equation on the profile of the co-dimension one hypersurface:

$$k + \lambda L^2 (k\mathcal{R} - 2k_{ij}\mathcal{R}^{ij}) + \frac{\lambda L^2}{3} (-k^3 + 3kk_{ij}k^{ij} - 2k_{il}k^{lj}k_j^i) = 0 \quad (7.13)$$

¹⁸We thank Aninda Sinha for pointing out these issues to us.

Although not equal, this equation bears a remarkable similarity with the divergent part of the qq -component (7.4) derived above from the conical boundary condition approach. While the first two terms in (7.13) are exactly the equation of motion derived from the Jacobson-Myers functional, the last term corresponds to the subleading term in (7.4). This means that from the discussion above, the additional closed extremal surfaces fail to satisfy (7.13) while only a black hole bifurcation surface would do so. For a spherical region on the boundary, the holographic entangling surfaces make the first two terms and the third term in (7.13) vanish separately. Hence they are extremal curves of the Jacobson-Myers functional and additionally satisfy the condition of third order in extrinsic curvature that we needed to rule out the additional closed extremal curves in the bulk. However, as mentioned in the above, the second term remains too restrictive for other boundary regions, such as a cylinder.

For NMG, in principle it is possible to perform analyses similar to those presented in this section, yet this is a very tedious task. Nevertheless, at least for the closed extremal curves presented in section 4.4 it would likely yield the same results. It was already mentioned in [12] that in cases with a full $U(1)$ symmetry in Euclidean time, the conical boundary conditions method reproduces Wald's entropy for Einstein-Hilbert gravity as well as for higher curvature theories.

8 Discussion

8.1 Summary

Let us begin this final section with a summary of this paper. We have investigated functional prescriptions of calculating entanglement entropy holographically in higher curvature gravity theories, using New Massive gravity (short NMG) and Gauss Bonnet gravity as concrete examples. We emphasised that in using entropy functionals to calculate entanglement entropy of a given region in a dual CFT, a non-trivial step is to find the particular surface upon which the corresponding functional is to be evaluated. The location of these surfaces can in principle be determined by solving the equations of motion with conical boundary conditions [12], however this is very involved and it is hoped that they could be alternatively determined by extremising the entropy functional [16]. In this work we considered the latter approach in (partially) static spacetimes (i.e. AdS and black hole backgrounds), introducing the RT-like and HRT-like prescriptions which are based on extremising the entropy functional (2.4) proposed for higher curvature theories of square order in the curvature. The RT-like prescription translates the Ryu and Takayanagi prescription for (partially) static spacetimes restricted to a constant time-slice in Einstein Hilbert gravity to higher curvature theories. The HRT-like prescription on the other hand is based on the Hubeny-Rangamani-Takayanagi prescription, which applies also to dynamical set ups. In both the RT- and HRT-like prescriptions, the extremal surfaces used to calculate CFT entropy holographically, for physicality, must be homologous to the full boundary. However in the HRT-like prescription, additional constraints can be imposed which arise from the Lorentzian nature of the spacetimes.

In a (partially) static scenario, the RT- and HRT-like prescriptions should agree, at least when a causality condition is imposed on the latter. To investigate this, we studied the nature of the extremal surfaces of the entropy functionals in NMG and Gauss-Bonnet gravity in sections 4 and 5 respectively. In particular we focused on closed extremal surfaces in AdS and black hole backgrounds, whose significance in relation to dual CFT entropy was explained in section 3. In black hole backgrounds, the bifurcation surface will always be a closed extremal surface of the entropy functional, however we discovered that for certain parameter ranges in NMG a closed extremal surface additional to the bifurcation surface also exists. For the non-rotating BTZ black hole background, this surface can encircle the black hole event horizon (see figures 5 and 6), and evaluates the entropy functional at a lower value than that given by the black hole bifurcation surface. As explained in sections 2 and 3, a naive implementation of the RT- and HRT-like proposals which employs only the homology constraint would hence require us to identify the CFT-entropy with the value given by the additional closed extremal surface, instead of the expected entropy.

Since NMG is plagued by several problems concerning unitarity in the bulk and on the boundary, in section 5 we investigated closed extremal surfaces for Gauss-Bonnet gravity, which is believed to be much better behaved and understood in a holographic context. We found that this theory also allows for additional closed bulk extremal surfaces, although for the rather unconventional choice of the Gauss-Bonnet coupling parameter $\lambda < 0$ (or $\lambda > 0$ in hyperbolic spacetimes). We found these additional extremal surfaces in topologically trivial spacetimes such as global AdS and boson stars. To us, our findings suggest that any functional of the type (2.4) that is complicated enough can in principle, at least for certain choices of the parameters, allow for additional closed bulk extremal curves.

This would have the implication that, when naively employing the prescriptions for calculating holographic entanglement entropy, the phenomenon of a seeming mismatch between CFT entropy and bulk entropy could be quite common in higher curvature theories. We hence adopted the view that the additional bulk extremal surfaces described above are unphysical.

In section 6 we therefore identified the strong form of the causal influence argument [27, 28] as a possible way to rule out the additional extremal surfaces encountered in this work. Nevertheless, this argument is intrinsically only applicable to entanglement entropy in an HRT-like approach, i.e. crucially it is only applicable in a Lorentzian setting. Since the additional extremal surfaces found appear in both Lorentzian and Euclidean settings, it would certainly be desirable to find a way to rule them out in an RT-like approach too.

In search of a means to dismiss the additional extremal surfaces in the RT-like approach, in section 7 for the example of Gauss-Bonnet gravity we turned to the alternative conical boundary condition method of finding entangling surfaces, based on translating the replica trick into the bulk [12]. Although it was argued in [16] that the equations of motion derived by extremising the functional (2.4) are equivalent to the conditions arising from the conical boundary condition method, we showed that this method has the potential to provide further conditions that rule out the additional closed extremal surfaces, leaving only the black hole bifurcation surface (if present) as the correct answer for the surface determining the full CFT entropy. However, as we noted there are examples where these additional

conditions seem to be too restrictive (e.g. a cylindrical entangling region in the boundary CFT). Further investigation into the application of these conditions would therefore be required.

8.2 Outlook

Spacetime from entanglement

We have given arguments throughout this work why the extremal surfaces additional to the black hole bifurcation surface should not be considered as defining the physical entanglement entropy of the CFT. Recently in [35] a number of results about entanglement entropy in the RT prescription for Einstein-Hilbert gravity with matter satisfying the null energy condition were proven. Amongst other properties, it was shown that in this case, the extremal surface computing the full CFT entropy will always be the bifurcation surface of the bulk event horizon, if it exists. Hence the existence of additional extremal surfaces is excluded in this setting. Although there is no straightforward generalisation of many of the proofs given in [35] to higher curvature theories and functionals of the form (2.4), it is interesting to note that the proof of the theorem mentioned above was the only one in that paper which made use of the equations of motion in Einstein-Hilbert gravity (and an energy condition on matter)¹⁹. In fact, our findings show that when varying functionals of the form (2.4) without imposing causality constraints (as proposed in [16]), this theorem does not generalise to higher curvature theories. We therefore think that this property is in fact the most non-trivial, and hence the physically most interesting of the results proven in [35]. In the past, ideas have been proposed that the holographic entangling surface \mathcal{E}_A and the homology surface \mathcal{F} corresponding to a boundary region A (see figure 1) define the part of the spacetime that can be holographically reconstructed from knowledge of the density matrix ρ_A , see [26, 35, 75]. In the framework of this conjecture, the additional extremal surfaces would be unphysical, as the corresponding homology surface \mathcal{F} would not reach as deep into the bulk as for the bifurcation surface, meaning that even full knowledge of the CFT would not be enough to reconstruct the entire spacetime from the boundary down to the event horizon.

ER=EPR

Another nice (but far from rigorous) argument against the validity of these additional extremal surfaces is the “ER=EPR” conjecture (see [76] and the ever growing list of papers citing this). It postulates a connection between non-traversable wormholes (ER) and entanglement (EPR), and is best explained for the example of an eternal black hole such as in figure 3. Here, the two CFTs are proposed to be in an entangled thermodouble state [77], and in the bulk their entanglement is supposed to be described by the presence of the Einstein-Rosen bridge (left side of figure 2). Concretely, the entanglement entropy between the two CFTs that can be calculated from the thermodouble state is equal to the bulk black hole entropy, given by the area of the bifurcation surface \mathcal{B} which is exactly the throat of the

¹⁹The same assumptions were made (amongst other technical details) in the proof of the causal influence argument presented in [28].

wormhole. If the additional closed extremal surfaces found in section 4.4 could not be ruled out, it would mean that the entanglement entropy between the two CFTs would no longer be equal to the black hole entropy. One might hope that the ER=EPR conjecture could at least still hold qualitatively in such cases, but even this is not true: While the existence of the bifurcation surface \mathcal{B} is intimately related to the presence of the wormhole and hence the topology of the spacetime, this is not the case for the additional closed extremal surfaces \mathcal{A} : As we argued in section 3, due to the flow of the Killing vector field ∂_t the bifurcation surface \mathcal{B} will always be an extremal surface of any functional, whereas additional curves \mathcal{A} only depend on the local geometry of the spacetime and the precise form of the entropy functional employed. From the perspective of ER=EPR, when the full spacetime contains a wormhole entanglement between the two asymptotic boundaries is connected to spacetime topology as well as to extremal surfaces.²⁰ As the additional extremal closed curves don't depend on the spacetime topology, and can even appear for topologically trivial spacetimes, they are not consistent with ER=EPR. Yet, as concluded in this paper, these curves can be ruled out for example by the causal influence argument.

Causality and other additional conditions

As explained in section 6, in a Lorentzian (HRT-like) setting the strong form of the causal influence argument elegantly rules out the additional extremal surfaces, at least for the examples considered in this paper. In that section we also pointed out that even in (partially) static spacetimes this argument implies that further restrictions should also be imposed in the RT-like approach if both are supposed to agree. It would hence be of great interest to better understand this argument, and whether it maybe is only the Lorentzian corollary of a more general restriction that has to be imposed both on HRT- and RT-like prescriptions. In section 7, we investigated whether for Gauss-Bonnet gravity in a Euclidean setting that such conditions might arise from an approach using conical boundary conditions. It would be interesting to find out whether such conditions for general surfaces and theories also have the effect of ruling out surfaces that would violate the causality condition in a Lorentzian setting. This would have the fascinating implication that the Euclidean computations already “know” in a sense about the causality in the Lorentzian setting.

$f(R)$ gravity

Another interesting model of higher curvature theories are $f(R)$ theories, where the gravitational Lagrangian is an arbitrary function of the Ricci scalar R . As pointed out in [16], using a field redefinition these theories can be mapped to Einstein-Hilbert gravity minimally coupled to a scalar field, where holographic entanglement entropy can be studied using the area functional (2.1). In this Einstein frame one can then apply the results of [35]. It would certainly be interesting to study whether $f(R)$ theories allow for additional extremal surfaces similarly to NMG and Gauss-Bonnet gravity, and how extremal surfaces

²⁰On the other hand, there do exist spacetimes where a bifurcation surface \mathcal{B} , and hence a non-traversable wormhole is present without having two asymptotic CFTs that might be entangled in an obvious way, for example the bag-of-gold spacetime. See: [25, 70, 71].

are mapped into the Einstein frame. This might shed some light on the conditions that have to be imposed on extremal surfaces in higher curvature theories.

9 Acknowledgements

We would like to thank Yves Brihaye, Betti Hartmann, Matthew Headrick, Aninda Sinha and Jia-ju Zhang for helpful correspondence, as well as Arpan Bhattacharyya, Ralph Blumenhagen, Olaf Hohm, Da-Wei Pang and Ivo Sachs for useful discussions. C.S. is grateful to Alejandra Castro, Jan Rosseel and Marika Taylor for interesting and helpful discussions. We would also like to thank Ann-Kathrin Straub, Migael Strydom and Hansjörg Zeller for comments on the draft.

A Notation

In this section we are going to clarify some of the notation used in this paper, especially in equation (2.4) that reads:

$$\mathcal{S}_{EE} = \frac{1}{4G_N} \int_{\Sigma} d^{d-1}y \sqrt{\gamma} \left[1 + 2aR + b \left(R_{\parallel} - \frac{1}{2}k^2 \right) + 2c (R_{\parallel\parallel} - \text{Tr}(k)^2) \right]$$

Here, Σ is a spacelike co-dimension two surface extending into the bulk. There are $d-1$ coordinates y^i on this surface, and the induced metric is γ_{ij} with determinant $\gamma > 0$.

Let us first give the definitions in case of a Euclidean bulk metric $g_{\mu\nu}$. Being co-dimension two, Σ has two normal vectors $n_{(\alpha)}^{\mu}$ with $\alpha \in \{1, 2\}$ and

$$n_{(1)}^{\mu} n_{(1)}^{\nu} g_{\mu\nu} = n_{(2)}^{\mu} n_{(2)}^{\nu} g_{\mu\nu} = +1, \quad n_{(1)}^{\mu} n_{(2)}^{\nu} g_{\mu\nu} = 0. \quad (\text{A.1})$$

We then define the projections

$$R_{\parallel} \equiv R_{\mu\nu} n_{(\alpha)}^{\mu} n_{(\alpha)}^{\nu}, \quad R_{\parallel\parallel} \equiv R_{\mu\rho\nu\sigma} n_{(\alpha)}^{\mu} n_{(\alpha)}^{\nu} n_{(\beta)}^{\rho} n_{(\beta)}^{\sigma} \quad (\text{A.2})$$

where double greek indices imply summation. The extrinsic curvature terms are defined via [14]

$$h_{\mu\nu} = g_{\mu\nu} - (n_{(\alpha)})_{\mu} (n_{(\alpha)})_{\nu} \quad (\text{A.3})$$

$$k_{\mu\nu}^{(\alpha)} = h_{\mu}^{\lambda} h_{\nu}^{\rho} (n_{(\alpha)})_{\lambda;\rho} \quad (\text{A.4})$$

$$k^2 = (k^{(\alpha)})_{\mu}^{\mu} (k^{(\alpha)})_{\nu}^{\nu} \quad (\text{A.5})$$

$$\text{Tr}(k)^2 = (k^{(\alpha)})_{\nu}^{\mu} (k^{(\alpha)})_{\mu}^{\nu}. \quad (\text{A.6})$$

For a Lorentzian bulk metric $g_{\mu\nu}$ these equations have to be modified as follows:

$$n_{(1)}^\mu n_{(1)}^\nu g_{\mu\nu} = -1, \quad n_{(2)}^\mu n_{(2)}^\nu g_{\mu\nu} = +1, \quad n_{(1)}^\mu n_{(2)}^\nu g_{\mu\nu} = 0 \quad (\text{A.7})$$

$$R_{||} \equiv R_{\mu\nu} n_{(\alpha)}^\mu n_{(\alpha)}^\nu = -R_{\mu\nu} n_{(1)}^\mu n_{(1)}^\nu + R_{\mu\nu} n_{(2)}^\mu n_{(2)}^\nu \quad (\text{similarly for } R_{|||}) \quad (\text{A.8})$$

$$h_{\mu\nu} = g_{\mu\nu} + (n_{(1)})_\mu (n_{(1)})_\nu - (n_{(2)})_\mu (n_{(2)})_\nu \quad (\text{A.9})$$

$$k_{\mu\nu}^{(\alpha)} = h_\mu^\lambda h_\nu^\rho (n_{(\alpha)})_{\lambda;\rho} \quad (\text{A.10})$$

$$k^2 = -(k^{(1)})_\mu^\mu (k^{(1)})_\nu^\nu + (k^{(2)})_\mu^\mu (k^{(2)})_\nu^\nu \quad (\text{A.11})$$

$$\text{Tr}(k)^2 = -(k^{(1)})_\nu^\mu (k^{(1)})_\mu^\nu + (k^{(2)})_\nu^\mu (k^{(2)})_\mu^\nu \quad (\text{A.12})$$

so that effectively the indices in brackets (like $(\dots)_{(\alpha)}$) are contracted with a Minkowski metric. This ensures that k^2 and $\text{Tr}(k)^2$ are independent of the choice of the $n_{(\alpha)}^\mu$ as long as $n_{(1)}^\mu$ is the timelike and $n_{(2)}^\mu$ is the spacelike normal vector.

B Explicit equations of motion for the entropy functional in NMG

In this section we will work with the (non-rotating) BTZ metric in Schwarzschild like coordinates:

$$g_{\mu\nu} = \begin{pmatrix} -M + \frac{r^2}{\ell^2} & 0 & 0 \\ 0 & \frac{1}{-M + \frac{r^2}{\ell^2}} & 0 \\ 0 & 0 & r^2 \end{pmatrix} \quad (\text{B.1})$$

As we are going to assume that the holographic entangling curves lie in an equal time slice of Schwarzschild time ($t = \text{const.}$, hence $r \geq \ell\sqrt{M}$), the sign of the g_{tt} -component and hence whether the metric is given in its Lorentzian or Euclidean form will not be relevant for us. The Lagrangian for a curve parameterised by $r = f(\phi)$, $t = \text{const.}$ then reads:

$$\mathcal{L} = \sigma \sqrt{f[\phi]^2 + \frac{f'[\phi]^2}{-M + \frac{f[\phi]^2}{\ell^2}}} \left(1 + \frac{1 - \ell^2 k^2}{2\sigma m^2 \ell^2} \right) \quad (\text{B.2})$$

with the extrinsic curvature term

$$k^2 = \frac{-1}{\ell^2 (M\ell^2 f[\phi]^2 - f[\phi]^4 - \ell^2 f'[\phi]^2)^3} \times \\ (-2M\ell^2 f[\phi]^4 + f[\phi]^6 - 2M\ell^4 f'[\phi]^2 + f[\phi]^2 (M^2\ell^4 + 3\ell^2 f'[\phi]^2) + M\ell^4 f[\phi] f''[\phi] - \ell^2 f[\phi]^3 f''[\phi])^2$$

Form this, we can derive the Euler-Lagrange equation of motion for $f(\phi)$, which takes the compact form

$$\begin{aligned}
0 = & -(M + 10m^2 M \ell^2 \sigma) f^{16} + 2m^2 \sigma f^{18} + (1 + 4m^2 \ell^2 \sigma) f^{14} (5M^2 \ell^2 + 3f'^2) + M \ell^2 (13 + 8m^2 \ell^2 \sigma) \\
& \times f^{13} f'' + M \ell^2 (13 + 8m^2 \ell^2 \sigma) f^{13} f'' - 2(1 + m^2 \ell^2 \sigma) f^{15} f'' - 60M^3 \ell^{10} f f'^4 f'' + M \ell^8 (41 + 2m^2 \ell^2 \sigma) \\
& \times f f'^6 f'' - \ell^2 f^{11} (32M^2 \ell^2 + 12m^2 M^2 \ell^4 \sigma + 111f'^2 + 6m^2 \ell^2 \sigma f'^2) f'' + 5\ell^4 f^9 f''^3 - 30M^2 \ell^{10} f f'^2 f''^3 \\
& + 15\ell^6 f^5 (M^2 \ell^2 - 2f'^2) f''^3 + 20M^2 \ell^{10} f f'^3 f'' f^{(3)} - \ell^2 f^{12} (10M^3 \ell^2 + 20m^2 M^3 \ell^4 \sigma + 27M f'^2 \\
& + 46m^2 M \ell^2 \sigma f'^2 - 15f''^2 - 20f' f^{(3)}) + \ell^4 f^9 f'' (38M^3 \ell^2 + 8m^2 M^3 \ell^4 \sigma + 347M f'^2 + 18m^2 M \ell^2 \sigma f'^2 \\
& + 20f' f^{(3)}) - 2M \ell^8 f'^4 (5f'^4 + 2m^2 \ell^2 \sigma f'^4 - 12M \ell^2 f''^2 + 4M \ell^2 f' f^{(3)}) - \ell^4 f^7 (22M^4 \ell^4 f'' \\
& + 2m^2 M^4 \ell^6 \sigma + 411M^2 \ell^2 f'^2 + 18m^2 M^2 \ell^4 \sigma f'^2 - 264f'^4 + 6m^2 \ell^2 \sigma f'^4 + 15M \ell^2 f''^2 + 60M \ell^2 f' f^{(3)}) \\
& - \ell^4 f^8 (5M^5 \ell^4 + 2m^2 M^5 \ell^6 \sigma + 93M^3 \ell^2 f'^2 + 42m^2 M^3 \ell^4 \sigma f'^2 + 237M f'^4 + 66m^2 M \ell^2 \sigma f'^4 \\
& - 72M^2 \ell^2 f''^2 + 135f'^2 f''^2 - 96M^2 \ell^2 f' f^{(3)}) + f^{10} (10M^4 \ell^6 + 10m^2 M^4 \ell^8 \sigma + 75M^2 \ell^4 f'^2 \\
& + 66m^2 M^2 \ell^6 \sigma f'^2 + 87\ell^2 f'^4 + 24m^2 \ell^4 \sigma f'^4 - 54M \ell^4 f''^2 - 72M \ell^4 f' f^{(3)}) + \ell^6 f^5 f'' (5M^5 \ell^4 \\
& + 225M^3 \ell^2 f'^2 + 6m^2 M^3 \ell^4 \sigma f'^2 - 525M f'^4 + 12m^2 M \ell^2 \sigma f'^4 + 60M^2 \ell^2 f' f^{(3)} + 20f'^3 f^{(3)}) + \ell^4 f^6 \\
& \times (M^6 \ell^6 + 54M^4 \ell^4 f'^2 + 10m^2 M^4 \ell^6 \sigma f'^2 + 289M^2 \ell^2 f'^4 + 60m^2 M^2 \ell^4 \sigma f'^4 - 175f'^6 + 20m^2 \ell^2 \sigma f'^6 \\
& - 42M^3 \ell^4 f''^2 + 342M \ell^2 f'^2 f''^2 - 56M^3 \ell^4 f' f^{(3)} - 4M \ell^2 f'^3 f^{(3)}) + \ell^6 f^2 f'^2 (46M^4 \ell^4 f'^2 - 89M^2 \ell^2 f'^4 \\
& + 14m^2 M^2 \ell^4 \sigma f'^4 + 21f'^6 + 6m^2 \ell^2 \sigma f'^6 + 72M^3 \ell^4 f''^2 - 84M \ell^2 f'^2 f''^2 - 4M^3 \ell^4 f' f^{(3)} \\
& + 28M \ell^2 f'^3 f^{(3)}) - \ell^6 f^3 f'' (50M^4 \ell^4 f'^2 - 321M^2 \ell^2 f'^4 + 6m^2 M^2 \ell^4 \sigma f'^4 + 47f'^6 + 2m^2 \ell^2 \sigma f'^6 \\
& + 5M^3 \ell^4 f''^2 - 60M \ell^2 f'^2 f''^2 + 20M^3 \ell^4 f' f^{(3)} + 40M \ell^2 f'^3 f^{(3)}) - \ell^6 f^4 (12M^5 \ell^4 f'^2 + 185M^3 \ell^2 f'^4 \\
& + 18m^2 M^3 \ell^4 \sigma f'^4 - 259M f'^6 + 34m^2 M \ell^2 \sigma f'^6 - 9M^4 \ell^4 f''^2 + 279M^2 \ell^2 f'^2 f''^2 - 60f'^4 f''^2 \\
& - 12M^4 \ell^4 f' f^{(3)} - 8M^2 \ell^2 f'^3 f^{(3)} + 20f'^5 f^{(3)}) - 2\ell^2 f (M^2 \ell^4 f^2 - 2M \ell^2 f^4 + f^6 - M \ell^4 f'^2 \\
& + \ell^2 f^2 f'^2)^2 f^{(4)}
\end{aligned} \tag{B.3}$$

C Closed extremal curves of other black hole solutions in NMG

For the more general rotating BTZ black hole we find through calculations similar to those done in section 4 (best performed in Eddington-Finkelstein coordinates [78]) additional extremal curves at radial distances

$$r_a^2 = \frac{M}{4\sigma m^2} \pm \frac{1}{4} \sqrt{\frac{M^2 - 6J^2 \sigma m^2}{m^4}} \tag{C.1}$$

for $\sigma m^2 < 0$, or when $\sigma m^2 > 0$ and $|J| < \sqrt{\frac{M^2}{6\sigma m^2}}$. As $r^2 > 0$, it depends on the values and signs of M, J, σ, m^2 which of the branches in (C.1) gives a valid solution.

One can also look at Lifshitz black holes [79]

$$g_{\mu\nu} = \begin{pmatrix} -\left(1 - \frac{M\ell^2}{r^2}\right) \frac{r^6}{\ell^6} & 0 & 0 \\ 0 & \frac{1}{\frac{r^2}{\ell^2} - M} & 0 \\ 0 & 0 & r^2 \end{pmatrix}. \tag{C.2}$$

which are solutions to NMG for $\ell^2 m^2 = -\frac{1}{2}$ and $\sigma = +1$. In this metric, additional extremal curves appear only for $M < 0$.

References

- [1] P. Calabrese and J. L. Cardy, *Entanglement entropy and quantum field theory*, *J.Stat.Mech.* **0406** (2004) P06002, [[hep-th/0405152](#)].
- [2] B. Swingle, *Entanglement renormalization and holography*, *Phys. Rev. D* **86** (Sep, 2012) 065007.
- [3] M. Van Raamsdonk, *Comments on quantum gravity and entanglement*, [arXiv:0907.2939](#).
- [4] J. M. Maldacena, *The Large N limit of superconformal field theories and supergravity*, *Adv.Theor.Math.Phys.* **2** (1998) 231–252, [[hep-th/9711200](#)].
- [5] S. Gubser, I. R. Klebanov, and A. M. Polyakov, *Gauge theory correlators from noncritical string theory*, *Phys.Lett.* **B428** (1998) 105–114, [[hep-th/9802109](#)].
- [6] E. Witten, *Anti-de Sitter space and holography*, *Adv.Theor.Math.Phys.* **2** (1998) 253–291, [[hep-th/9802150](#)].
- [7] J. D. Bekenstein, *Black holes and entropy*, *Phys.Rev.* **D7** (1973) 2333–2346.
- [8] S. Hawking, *Particle Creation by Black Holes*, *Commun.Math.Phys.* **43** (1975) 199–220.
- [9] A. Strominger and C. Vafa, *Microscopic origin of the Bekenstein-Hawking entropy*, *Phys.Lett.* **B379** (1996) 99–104, [[hep-th/9601029](#)].
- [10] S. Ryu and T. Takayanagi, *Holographic derivation of entanglement entropy from AdS/CFT*, *Phys.Rev.Lett.* **96** (2006) 181602, [[hep-th/0603001](#)].
- [11] S. Ryu and T. Takayanagi, *Aspects of Holographic Entanglement Entropy*, *JHEP* **0608** (2006) 045, [[hep-th/0605073](#)].
- [12] A. Lewkowycz and J. Maldacena, *Generalized gravitational entropy*, *JHEP* **1308** (2013) 090, [[arXiv:1304.4926](#)].
- [13] V. E. Hubeny, M. Rangamani, and T. Takayanagi, *A Covariant holographic entanglement entropy proposal*, *JHEP* **0707** (2007) 062, [[arXiv:0705.0016](#)].
- [14] D. V. Fursaev, A. Patrushev, and S. N. Solodukhin, *Distributional Geometry of Squashed Cones*, *Phys.Rev.* **D88** (2013) 4, 044054, [[arXiv:1306.4000](#)].
- [15] R.-X. Miao, *A Note on Holographic Weyl Anomaly and Entanglement Entropy*, *Class. Quant. Grav.* **31** (2014) 065009, [[arXiv:1309.0211](#)].
- [16] X. Dong, *Holographic Entanglement Entropy for General Higher Derivative Gravity*, *JHEP* **1401** (2014) 044, [[arXiv:1310.5713](#)].
- [17] J. Camps, *Generalized entropy and higher derivative Gravity*, *JHEP* **1403** (2014) 070, [[arXiv:1310.6659](#)].
- [18] R. M. Wald, *Black hole entropy is the Noether charge*, *Phys.Rev.* **D48** (1993) 3427–3431, [[gr-qc/9307038](#)].
- [19] T. Jacobson, G. Kang, and R. C. Myers, *On black hole entropy*, *Phys.Rev.* **D49** (1994) 6587–6598, [[gr-qc/9312023](#)].

- [20] V. Iyer and R. M. Wald, *Some properties of Noether charge and a proposal for dynamical black hole entropy*, *Phys.Rev.* **D50** (1994) 846–864, [[gr-qc/9403028](#)].
- [21] L.-Y. Hung, R. C. Myers, and M. Smolkin, *On Holographic Entanglement Entropy and Higher Curvature Gravity*, *JHEP* **1104** (2011) 025, [[arXiv:1101.5813](#)].
- [22] E. Witten, *Anti-de Sitter space, thermal phase transition, and confinement in gauge theories*, *Adv.Theor.Math.Phys.* **2** (1998) 505–532, [[hep-th/9803131](#)].
- [23] S. Banerjee, A. Bhattacharyya, A. Kaviraj, K. Sen and A. Sinha, *Constraining gravity using entanglement in AdS/CFT*, *JHEP* **1405** (2014) 029, [[arXiv:1401.5089](#)].
- [24] D. V. Fursaev, *Proof of the holographic formula for entanglement entropy*, *JHEP* **0609** (2006) 018, [[hep-th/0606184](#)].
- [25] V. E. Hubeny, H. Maxfield, M. Rangamani, and E. Tonni, *Holographic entanglement plateaux*, *JHEP* **1308** (2013) 092, [[arXiv:1306.4004](#)].
- [26] A. C. Wall, *Maximin Surfaces, and the Strong Subadditivity of the Covariant Holographic Entanglement Entropy*, [arXiv:1211.3494](#).
- [27] M. Headrick, *What can entanglement entropy teach us about general relativity?*, 19 September 2013. Talk given at Newton Institute, see <http://www.newton.ac.uk/programmes/HOL/seminars/2013091914001.html> or <http://people.brandeis.edu/~headrick/EEGR.pdf>.
- [28] M. Headrick, V. E. Hubeny, A. Lawrence, and M. Rangamani, “Causality and holographic entanglement entropy.” To appear.
- [29] E. A. Bergshoeff, O. Hohm, and P. K. Townsend, *Massive Gravity in Three Dimensions*, *Phys.Rev.Lett.* **102** (2009) 201301, [[arXiv:0901.1766](#)].
- [30] E. A. Bergshoeff, O. Hohm, and P. K. Townsend, *More on Massive 3D Gravity*, *Phys.Rev.* **D79** (2009) 124042, [[arXiv:0905.1259](#)].
- [31] D. Lovelock, *The Einstein tensor and its generalizations*, *J.Math.Phys.* **12** (1971) 498–501.
- [32] T. Padmanabhan and D. Kothawala, *Lanczos-Lovelock models of gravity*, *Phys.Rept.* **531** (2013) 115–171, [[arXiv:1302.2151](#)].
- [33] V. E. Hubeny and M. Rangamani, *Causal Holographic Information*, *JHEP* **1206** (2012) 114, [[arXiv:1204.1698](#)].
- [34] M. Headrick and T. Takayanagi, *A Holographic proof of the strong subadditivity of entanglement entropy*, *Phys.Rev.* **D76** (2007) 106013, [[arXiv:0704.3719](#)].
- [35] M. Headrick, *General properties of holographic entanglement entropy*, *JHEP* **1403** (2014) 085, [[arXiv:1312.6717](#)].
- [36] Y. Liu and Y.-w. Sun, *Note on New Massive Gravity in AdS(3)*, *JHEP* **0904** (2009) 106, [[arXiv:0903.0536](#)].
- [37] D. Grumiller and O. Hohm, *AdS(3)/LCFT(2): Correlators in New Massive Gravity*, *Phys.Lett.* **B686** (2010) 264–267, [[arXiv:0911.4274](#)].
- [38] Y. Liu and Y.-W. Sun, *Consistent Boundary Conditions for New Massive Gravity in AdS₃*, *JHEP* **0905** (2009) 039, [[arXiv:0903.2933](#)].
- [39] U. Camara dS, C. Constantinidis, and G. Sotkov, *New Massive Gravity Holography*, *Int.J.Mod.Phys.* **A28** (2013) 1350073, [[arXiv:1009.2665](#)].

- [40] A. Sinha, *On the new massive gravity and AdS/CFT*, *JHEP* **1006** (2010) 061, [[arXiv:1003.0683](#)].
- [41] B. Chen, J.-j. Zhang, J.-d. Zhang, and D.-l. Zhong, *Aspects of Warped AdS₃/CFT₂ Correspondence*, *JHEP* **1304** (2013) 055, [[arXiv:1302.6643](#)].
- [42] M. Alishahiha, A. F. Astaneh, and M. R. M. Mozaffar, *Entanglement Entropy for Logarithmic Conformal Field Theory*, *Phys.Rev.* **D89** (2014) 065023, [[arXiv:1310.4294](#)].
- [43] B. Chen, F.-y. Song, and J.-j. Zhang, *Holographic Rényi entropy in AdS₃/LCFT₂ correspondence*, *JHEP* **1403** (2014) 137, [[arXiv:1401.0261](#)].
- [44] J. D. Brown and M. Henneaux, *Central Charges in the Canonical Realization of Asymptotic Symmetries: An Example from Three-Dimensional Gravity*, *Commun.Math.Phys.* **104** (1986) 207–226.
- [45] P. Kraus and F. Larsen, *Microscopic black hole entropy in theories with higher derivatives*, *JHEP* **0509** (2005) 034, [[hep-th/0506176](#)].
- [46] M. Banados, M. Henneaux, C. Teitelboim, and J. Zanelli, *Geometry of the (2+1) black hole*, *Phys.Rev.* **D48** (1993) 1506–1525, [[gr-qc/9302012](#)].
- [47] M. Banados, C. Teitelboim, and J. Zanelli, *The Black hole in three-dimensional space-time*, *Phys.Rev.Lett.* **69** (1992) 1849–1851, [[hep-th/9204099](#)].
- [48] A. Bhattacharyya, M. Sharma, and A. Sinha, *On generalized gravitational entropy, squashed cones and holography*, *JHEP* **1401** (2014) 021, [[arXiv:1308.5748](#)].
- [49] H. Casini, M. Huerta, and R. C. Myers, *Towards a derivation of holographic entanglement entropy*, *JHEP* **1105** (2011) 036, [[arXiv:1102.0440](#)].
- [50] J. de Boer, M. Kulaxizi, and A. Parnachev, *Holographic Entanglement Entropy in Lovelock Gravities*, *JHEP* **1107** (2011) 109, [[arXiv:1101.5781](#)].
- [51] X. O. Camanho, J. D. Edelstein, and J. M. S. de Santos, *Lovelock theory and the AdS/CFT correspondence*, *Gen.Rel.Grav.* **46** (2014) 1637, [[arXiv:1309.6483](#)].
- [52] J. D. Edelstein, *Lovelock theory, black holes and holography*, [[arXiv:1303.6213](#)].
- [53] M. Brigante, H. Liu, R. C. Myers, S. Shenker, and S. Yaida, *Viscosity Bound Violation in Higher Derivative Gravity*, *Phys.Rev.* **D77** (2008) 126006, [[arXiv:0712.0805](#)].
- [54] M. Brigante, H. Liu, R. C. Myers, S. Shenker, and S. Yaida, *The Viscosity Bound and Causality Violation*, *Phys.Rev.Lett.* **100** (2008) 191601, [[arXiv:0802.3318](#)].
- [55] A. Buchel and R. C. Myers, *Causality of Holographic Hydrodynamics*, *JHEP* **0908** (2009) 016, [[arXiv:0906.2922](#)].
- [56] D. M. Hofman, *Higher Derivative Gravity, Causality and Positivity of Energy in a UV complete QFT*, *Nucl.Phys.* **B823** (2009) 174–194, [[arXiv:0907.1625](#)].
- [57] D. G. Boulware and S. Deser, *String Generated Gravity Models*, *Phys.Rev.Lett.* **55** (1985) 2656.
- [58] T. Jacobson and R. C. Myers, *Black hole entropy and higher curvature interactions*, *Phys.Rev.Lett.* **70** (1993) 3684–3687, [[hep-th/9305016](#)].
- [59] J. T. Wheeler, *Symmetric Solutions to the Gauss-Bonnet Extended Einstein Equations*, *Nucl.Phys.* **B268** (1986) 737.

- [60] J. T. Wheeler, *Symmetric Solutions to the Maximally Gauss-Bonnet Extended Einstein Equations*, *Nucl.Phys.* **B273** (1986) 732.
- [61] R.-G. Cai, *Gauss-Bonnet black holes in AdS spaces*, *Phys.Rev.* **D65** (2002) 084014, [[hep-th/0109133](#)].
- [62] X. O. Camanho and J. D. Edelstein, *A Lovelock black hole bestiary*, *Class. Quant. Grav.* **30** (2013) 035009, [[arXiv:1103.3669](#)].
- [63] T. Torii and H. Maeda, *Spacetime structure of static solutions in Gauss-Bonnet gravity: Charged case*, *Phys.Rev.* **D72** (2005) 064007 [[hep-th/0504141](#)].
- [64] B. Hartmann, Jür. Riedel and R. Suci, *Gauss-Bonnet boson stars*, *PhysLett.* **B 726** (2013) 906 [[arXiv:1308.3391](#)].
- [65] L. J. Henderson, R. B. Mann and S. Stotyn, *Gauss-Bonnet Boson Stars with a Single Killing Vector*, [arXiv:1403.1865](#).
- [66] H. Araki and E. Lieb, *Entropy inequalities*, *Commun.Math.Phys.* **18** (1970) 160–170.
- [67] A. Bhattacharyya, A. Kaviraj, and A. Sinha, *Entanglement entropy in higher derivative holography*, *JHEP* **1308** (2013) 012, [[arXiv:1305.6694](#)].
- [68] B. Chen and J.-j. Zhang, *Note on generalized gravitational entropy in Lovelock gravity*, *JHEP* **07** (2013) 185, [[arXiv:1305.6767](#)].
- [69] S. S. Pal, *Extremal Surfaces And Entanglement Entropy*, *Nucl.Phys.* **B882** (2014) 352, [[arXiv:1312.0088](#)].
- [70] B. Freivogel, V. E. Hubeny, A. Maloney, R. C. Myers, M. Rangamani, et al., *Inflation in AdS/CFT*, *JHEP* **0603** (2006) 007, [[hep-th/0510046](#)].
- [71] D. Marolf, *Black Holes, AdS, and CFTs*, *Gen.Rel.Grav.* **41** (2009) 903–917, [[arXiv:0810.4886](#)].
- [72] V. E. Hubeny, M. Rangamani, and E. Tonni, *Global properties of causal wedges in asymptotically AdS spacetimes*, *JHEP* **1310** (2013) 059, [[arXiv:1306.4324](#)].
- [73] T. Jacobson, *When is $g(tt)g(rr) = -1$?*, *Class.Quant.Grav.* **24** (2007) 5717–5719, [[arXiv:0707.3222](#)].
- [74] A. Bhattacharyya and A. Sinha, *Entanglement entropy from the holographic stress tensor*, *Class.Quant.Grav.* **30** (2013) 235032, [[arXiv:1303.1884](#)].
- [75] B. Czech, J. L. Karczmarek, F. Nogueira, and M. Van Raamsdonk, *The Gravity Dual of a Density Matrix*, *Class.Quant.Grav.* **29** (2012) 155009, [[arXiv:1204.1330](#)].
- [76] J. Maldacena and L. Susskind, *Cool horizons for entangled black holes*, *Fortsch. Phys.* **61** (2013) 781, [[arXiv:1306.0533](#)].
- [77] J. M. Maldacena, *Eternal black holes in anti-de Sitter*, *JHEP* **0304** (2003) 021, [[hep-th/0106112](#)].
- [78] J. Chan, K. Chan, and R. B. Mann, *Interior structure of a charged spinning black hole in $(2+1)$ -dimensions*, *Phys.Rev.* **D54** (1996) 1535–1539, [[gr-qc/9406049](#)].
- [79] E. Ayon-Beato, A. Garbarz, G. Giribet, and M. Hassaine, *Lifshitz Black Hole in Three Dimensions*, *Phys.Rev.* **D80** (2009) 104029, [[arXiv:0909.1347](#)].